Aus der Neurologischen Klinik und Poliklinik
Der Universität Würzburg
Direktor: Prof. Dr. med. J. Volkmann

CSF-1 receptor as a target for the treatment of Charcot-Marie-Tooth disease 1

Inaugural – Dissertation
zur Erlangung der Doktorwürde
der Medizinischen Fakultät
der
Julius-Maximilians-Universität Würzburg

vorgelegt von
ÁgnesPatzkó
aus Gyenesdiás, Ungarn

Würzburg, Oktober 2012

Referent: Prof. Dr. rer. nat. R. Martini

Koreferentin: Prof. Dr. med. E. Asan

Dekan: Prof. Dr. Matthias Frosch

Tag der mündlichen Prüfung: 18.07.2013

Die Promovendin ist Ärztin.

Für
meine Eltern und meinen Mann

Az elsőtalálkozás a tudománnyal olyan részegítő,
mint a szerelem.

Antal Szerb

Table of Contents

1. Introduction

1.1 Charcot-Marie-Tooth disease

1.1.1. Clinical aspects of Charcot-Marie-Tooth disease

Charcot-Marie-Tooth disease (CMT), also known as hereditary motor and sensory neuropathy (HMSN)/ hereditary sensorimotor neuropathy (HSMN) or peroneal muscular atrophy, is one of the most common inherited neurologic disorders with an estimated prevalence of 1:2500 (Skre, 1974). This disease entity was first described in the late 19th century by Charcot and Marie (1886) in France and independently by Tooth (1886) in England, hence the name of the disease. Later on Dejerine and Sottas (1893) introduced subjects that were more severely affected and had an onset in infancy; and Roussy and Levy (1926) reported cases associated with tremor, ataxia, areflexia, and pes cavus. Early studies suggested that most patients with CMT could be divided into one group with slow nerve conduction velocities (NCV) (<38 m/s) and pathologic evidence of a hypertrophic demyelinating neuropathy (CMT type 1) and a second group with relatively normal nerve conduction velocities and axonal degeneration (CMT type 2) (Dyck and Lambert, 1968; Harding and Thomas, 1980a, b). The classification of this clinically diverse disorder with overlapping phenotypes has become complex. CMT is subdivided based on the inheritance pattern, neurophysiologic criteria and the causal mutations **(Table 1)**. Major categories include CMT1 (autosomal dominant/X-linked demyelinating CMT), CMT2 (autosomal dominant axonal CMT), Dejerine-Sottas syndrome and congenital hypomyelinating neuropathy (severe infantile onset) and CMT4 (autosomal recessive CMT).

In North-America and most parts of Europe more than 90% of CMT cases result from autosomal dominant and X-linked CMT (Reilly and Shy, 2009); whereas in countries with a higher rate of consanguineous marriages, autosomal recessive forms are responsible for about 40% of CMT cases (Dubourg et al., 2006). CMT1 is the most common form in most regions of the world and CMT1A alone accounts for 70% of CMT1 cases (Nelis et al., 1996). The description below focuses on the frequent forms of CMT, especially on demyelinating CMT1; rare causes are listed in **Table 1**.

CMT1 patients usually present with a ‘‘classical CMT phenotype’’ meaning a slowly progressive, symmetrical, length dependent neuropathy that begins in the first two decades of life but does not shorten lifespan. Motor symptoms predominantly affect the distal leg, leading to foot drop and difficulty walking, ankle sprains, frequent tripping and falling associated with weakness, muscle wasting and decreased or absent deep tendon reflexes. Skeletal abnormalities resulting from CMT are high arches (pes cavus) or flat foot, hammer toes and scoliosis **(Figure 1)**. Patients often need ankle-foot orthotics, but rarely become wheelchair bound. Proximal muscles and hands are less affected or become involved later during the course of the disease **(Figure 1)**. Sensation is decreased distally, and patients experience numbness and paresthesias; however, the latter are generally not the presenting symptoms of the disorder. Additional symptoms include impaired balance, muscle cramps, musculoskletal and neuropathic pain, exhaustion, cold extremities and rarely, enlarged palpable nerves. Median and ulnar motor NCVs are below 38 m/s, and sensory action potentials are either reduced or absent. A nerve biopsy demonstrates demyelination and onion bulb formation, but this is not necessary to make the diagnosis.

CMT1B, caused by a mutation in *myelin protein zero* (*MPZ*), accounts for about 10% of CMT1. Most patients can be separated into two distinct phenotypes: a severe, early-onset form with delayed walking and NCV less than 10 m/s or a late-onset mild axonal neuropathy (Shy et al., 2004); nevertheless, few patients present with the ‘classical CMT phenotype’.

CMT1X represents the second most frequent form of CMT and results from mutations in the *gap junction protein beta1* (*GJB1*) gene encoding connexin 32 (Cx32) (Bergoffen et al., 1993). So far more than 300 amino acid changing mutations have been described in this gene that are virtually all pathogenic; and most male patients have a corresponding phenotype to patients with a complete deletion of the gene. Males are usually more impaired than female patients, but due to random X inactivation females may present with a variety of symptoms (Siskind et al., 2011). NCVs are in the intermediate range (25–40 m/s) in both men and women (Lewis and Shy, 1999). Asymmetric presentation, intrinsic hand muscle atrophy and sensory symptoms may be more common than in other subtypes. Central nervous system (CNS) involvement has been described in rare cases (mild deafness, abnormal brainstem-evoked potentials) (Kleopa et al., 2002), but

occasionally can be transiently debilitating, causing ataxia and dysarthria (Paulson et al., 2002; Taylor et al., 2003).

Hereditary neuropathy with liability to pressure palsy (HNPP) is an autosomal dominantly inherited disorder that usually starts in the second or third decade. It is often evoked by compression or repetitive use of the affected limbs resulting in dysfunction of individual nerves or plexus, leading to transient focal weakness or sensory loss. Two common presenting symptoms are carpal tunnel syndrome and peroneal palsy with foot drop. Focal areas of slowing around sites of compression can often be seen in neurophysiological studies (Li et al., 2002).

Figure 1. Clinical features of Charcot-Marie-Tooth disease.

A) and B) Moderate to severe foot deformities in CMT1A (pes cavus, hammer toes, and callosities). **C) and D)** Wasting of hand muscles. **E)** Patient with CMT1A; note pes cavus, the moderate wasting of leg muscles and of the lower third of the thigh. **F)** Patient with late-onset CMT2 associated with an *MPZ* gene mutation. Foot drop, severe wasting of lower limb muscles, no evidence of foot deformities [(Pareyson et al., 2006) Copyright obtained from Springer].

Most CMT2 patients present with the "classical phenotype," but have a wider range of age of onset than CMT1A patients. NCVs in the upper extremities are greater than 38 m/s and compound muscle action potential (CMAP) amplitudes are reduced, sometimes even unobtainable in severely affected patients. To date, causative mutations have been identified in 25% to 35% of CMT2 cases, with CMT2A accounting for 20% of all CMT2 cases. Most CMT2A patients are characterized by a severe, early-onset impairment (Feely et al., 2011). Occasionally optic atrophy, brisk reflexes and minor white matter changes occur (Zuchner and Vance, 2006). Specific features of less common CMT2 subtypes include sensory involvement and complications (e.g.: ulceromutilations) in CMT2B, vocal cord and respiratory involvement in CMT2C, hand wasting and weakness in CMT2D, early onset and slow NCVs in CMT2E.

Dejerine-Sottas syndrome (DSS) and congenital hypomyelinating neuropathy (CHN) refer to genetic neuropathies that begin in infancy. Mutations in *MPZ*, *peripheral myelin protein 22* (*PMP22)*, *early growth response 2* (*EGR2)*, and *periaxin* (*PRX)* can be the underlying cause. These severe cases used to be labeled as CMT3 and were thought to be inherited in a recessive manner. However, the old classification did not hold true (recessive disorders are now classified as CMT4); some new or dominantly inherited mutations can also result in a severe phenotype corresponding to DSS or CHN. The two disorders might partially overlap and it may be challenging to distinguish them. Patients classified as having either CHN or DSS have shown the same severe pathological changes on sural nerve biopsies. Both disorders are associated with early onset, delayed motor skills, very slow NCV (less than 10 m/s) and might mean a life threatening condition due to respiratory failure in infancy. Patients with DSS have severe sensory and skeletal deficits with extension to proximal muscles, sensory ataxia, and scoliosis and mostly become wheelchair bound. Patients with CHN are usually hypotonic and areflexic in the first year of life and might present with arthrogryposis [reviewed in (Reilly and Shy, 2009)].

Most forms of autosomal recessive CMT4 belong to demyelinating neuropathies, but mutations in 2 genes (*LMNA and GDAP1*) can result in axonal neuropathy. Patients are usually severely affected; infantile onset and the involvement of proximal muscles are typical and often lead to the loss of ambulation. The diagnosis of CMT4 can be challenging. On one hand polymorphisms are frequent and compound heterozygous mutations can be disease causing. On the other hand potentials are often unobtainable at routine recording sites, conduction studies of proximal

segments may be necessary to identify demyelination. Nerve biopsy can be of great diagnostic value; specific features seen in the sample are highly suggestive of certain mutations (Bernard et al., 2006).

Several international guidelines, including a recently published practice parameter (England et al., 2009a, b) facilitate a more effective diagnosis of CMT. Among others, they propose an algorithm focusing genetic testing based on the prevalence of CMT types, whether NCV is reduced, and whether or not there was a family history of neuropathy. Currently there is no cure available for CMT; but genetic counseling, symptomatic and rehabilitative treatment are essential in the management of patients.

1.1.2. Molecular aspects of Charcot-Marie-Tooth disease

CMT encompasses a genetically heterogeneous group of disorders that results from mutations in more than 40 genes **(Table 1)**. In spite of the broad spectrum of genes involved in the pathogenesis, common molecular pathways have been discovered **(Figure 2)**. These include transcriptional regulation, protein turnover, Schwann cell - axonal interactions, axonal transport, mitochondrial fusion and fission, and a chronic, low grade inflammation. Some causal mutations are found in PNS-specific proteins (PMP22, MPZ, periaxin), whereas other genes (*GJB1, GARS, HS27*) encode widely expressed proteins that previously were not known to have a PNS-specific role, but that lead to peripheral neuropathy. Some mutations, most notably in *MPZ, GJB1*, but also in *GDAP1, NF-L* and *DNM2* can result in either demyelinating or axonal neuropathies; moreover, they can lead to axonal damage even if the primary defect caused by the mutation is Schwann-cell-autonomous. This fact underlines the importance of intimate Schwann cell – axonal connection, which probably explains the debilitating secondary axonal damage seen in primarily demyelinating neuropathies caused by *MPZ* and *GJB1* mutations. The following paragraphs and chapters are going to focus on pathomechanisms related to demyelinating forms of CMT and only briefly mention other aspects.

Table 1. Classification of Charcot-Marie-Tooth disease.

Adapted from (Patzkó, 2012)

Type	Subtype	Gene	Locus
Autosomal dominant demyelinating CMT (CMT1)	CMT1A	*PMP22 (peripheral myelin protein22)*	Dup 17p 11
	CMT1B	*MPZ (myelin protein zero)*	1q22
	CMT1C	*LITAF (lipopolysaccharide-induced TNF factor)*	16p13
	CMT1D	*EGR2 (early growth response 2)/Krox-20*	10q21
	CMT1E	*PMP22 point mutations*	17p11
	CMT1F	*NEFL (neurofilament light chain)*	8q21
X-linked demyelinating CMT(CMT1)	CMT1X	*GJB1 (gap junction protein beta 1)*	Xq13
	CMTX2		Xq22
	CMTX3		Xq26
	CMTX4		Xq24-26
	CMTX5		Xq22-24
Autosomal dominant axonal CMT (CMT2)	CMT2A	*MFN2 (mitofusin-2)*	1p36
	CMT2B	*RAB7(Rab family of Ras GTPases)*	3q21
	CMT2C	*TRPV4 (Transient receptor potential cation channel subfamily V member 4)*	12q23-q24
	CMT2D	*GARS (glycyl-tRNA synthetase)*	7p15
	CMT2E	*NEFL*	8p21
	CMT2F	*HSP27 (HSPB1)(27 kDa small heat-shock proteinB1)*	7q11
	CMT2G		12q12–q13.3
	CMT2J	*MPZ*	1q22
	CMT2L	*HSP22 (HSPB8)(22 kDa small heat-shock proteinB8)*	12q24
	CMT2N	*AARS (alanyl-tRNA synthetase)*	16q22.1
	CMT2 (HMSNP)		3q13.1
Autosomal recessive axonal CMT (AR-CMT2/CMT4)	CMT2A	*LMNA (lamin A/C)*	1q21
	CMT2B		19q13.1–13.3
	CMT2H	*GDAP1(ganglioside-induced differentiation-associated protein 1)*	8q13
	CMT2K	*GDAP1*	8q13
Autosomal recessive demyelinating CMT (CMT4)	CMT4A	*GDAP1*	8q13
	CMT4B1	*MTMR2 (myotubularin related protein 2)*	11q22
	CMT4B2	*MTMR13/SBF2 (myotubularin related protein 13/set binding factor 2)*	11p15
	CMT4C	*KIAA1985 (SH3TC2) (Src homology 3 domain and tetratricopeptide repeats 2)*	5q32
	CMT4D	*NDRG1 (N-myc downstream regulated 1)*	8q24
	CMT4E	*EGR2*	10q21
	CMT4F	*PRX (periaxin)*	19q13
	CMT4H	*FGD4 (actin-filament binding protein frabin)*	12p11.21
	CMT4J	*FIG4 (phosphatidylinositol 3,5-bisphosphate 5-phosphatase)*	6q21
	CCFDN	*CTDP1 (carboxy-terminal domain, RNA polymerase II, polypeptide A phosphatase, subunit 1)*	18q
	HMSN Russe		10q22–q23
	CMT1	*PMP22 (point mutation)*	17p11
	CMT1	*MPZ*	1q22
Dominant intermediate CMT (DI-CMT)	CMTA		10q24.1–25.1
	CMTB	*DNM2 (dynamin 2)*	19p12
	CMTC	*YARS (tyrosyl-tRNA synthetase)*	1p34
Hereditary neuropathy with liability to pressure palsy (HNPP)		*PMP-22* *PMP22* (point mutation)	Del 17p11

The most common form of CMT is caused by a 1.4 Mb duplication on chromosome 17 in the region carrying *PMP22* (Lupski et al., 1991; Raeymaekers et al., 1991); conversely the deletion of the same region leads to HNPP (Chance et al., 1993). Thus, alterations of *PMP22* gene dosage result in two different disease entities. The hypothesis that the precise stoichiometry of PMP22 is required (Suter and Snipes, 1995) remains plausible and has been targeted in several studies altering PMP22 mRNA levels. Administration of a selective progesterone receptor antagonist (onapristone) or ascorbic acid improved the phenotype of CMT1A animal models and reduced PMP22 mRNA levels (Passage et al., 2004; Meyer zu Horste et al., 2007). Unfortunately, progesterone antagonists are too toxic for human use and clinical trials with ascorbic acid could not provide evidence of a beneficial effect in patients suffering from CMT1A (Burns et al., 2009b; Micallef et al., 2009; Verhamme et al., 2009; Pareyson et al., 2011). Besides the gene dosage, the regulation of PMP22 levels appears to be complex. PMP22 has a short half-life (Notterpek et al., 1999) and up to 90% of translated PMP22 is degraded through the ubiquitin-proteosome pathway before reaching the myelin sheath (Pareek et al., 1997).

Protein misfolding and impaired protein or membrane trafficking are also common mechanisms of high importance **(Figure 2)**. Both P0 and PMP22 are synthesized and glycosylated in the endoplasmic reticulum (ER) and then transported through the Golgi apparatus to the cell surface. *PMP22* missense mutations Leu16Pro (Valentijn et al., 1992) and Leu147Arg (Navon et al., 1996) cause a dysmyelinating neuropathy in humans and naturally occurring trembler J (TrJ) (Suter et al., 1992a) and trembler (Tr) (Suter et al., 1992b) mouse mutants. While wild-type Pmp22 is transported to the compact myelin, both Tr and TrJ are retained in the ER (Colby et al., 2000) and lead to a more severe neuropathy than HNPP (where PMP22 protein levels are reduced to 50%). Therefore the mutant PMP22 must not only result in reduced functional PMP22 (as in case of HNPP) but also act through an abnormal gain of function mechanism due the negative consequences of protein retention in the ER. Recent in vitro and in vivo studies showed that mutant MPZ could also accumulate in the ER and elicit the unfolded protein response (Pennuto et al., 2008). Even when the mutated protein is transported to the cell surface and is incorporated into myelin it may disrupt this structure, presumably by dominant-negative interactions between the mutated and wild-type P0 (Previtali et al., 2000).

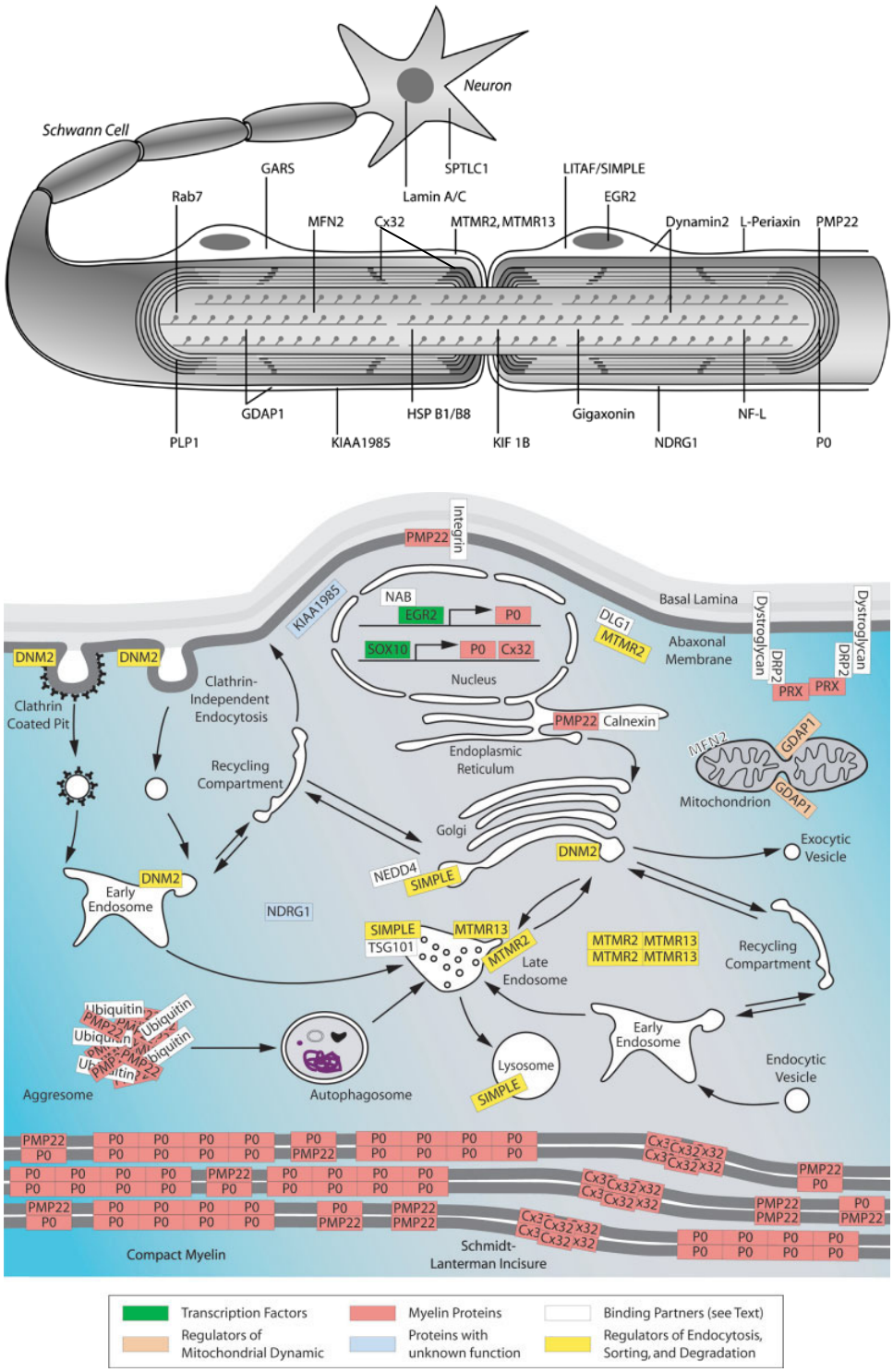

Figure 2. Schematic representation of proteins and intracellular pathways that are involved in the pathogenesis of CMT.

Note, that P0 and PMP22 are localized to compact myelin, while Cx32 is found in non-compact myelin. Major CMT1 relevant pathomechanisms are discussed below [modified from (Berger et al., 2006; Niemann et al., 2006)]. Modification: Indication that Cx32 is also present in the paranodal loops.

Protein turnover from the cell surface to the lysosome appears to play an important role in CMT1C (*LITAF/SIMLE* mutation) (Street et al., 2003) and CMT2B (Rab7 mutation) (Verhoeven et al., 2003) which result from the impairment of lysosomal transport or degradation. Mutations in myotubularin-related proteins (MTMR) 2 and 13 and in *FIG4* cause CMT4B1, CMT4B2, and CMT4J respectively, by disrupting phosphoinositol-mediated trafficking of vesicles within the cell (Senderek et al., 2003; Chow et al., 2007). Impaired trafficking of GJB1 mutants has also been described. Some of the more than 300 disease-associated mutants form fully functional channels, but many others result in nonfunctional channels or in functional channels with altered biophysical characteristics. How these mutations lead to demyelination has not yet been completely elucidated.

Mutations affecting two promyelinating transcription factors, EGR2/Krox20 and Sox10, have been associated with CMT. EGR/Krox20 is one of the major regulators of myelination, mutations in this gene cause demyelinating or dysmyelinating forms of CMT (CMT1D, CMT4E, and CHN). Surprisingly, two CMT1X-causing mutations impair SOX10 function on the mutated P2 promoter of Cx32/*GJB1* (Bondurand et al., 2001; Houlden et al., 2004).

Mitochondrial transport provides essential energy support to distal axons that are far away from their cell body. Mutations in mitochondrial proteins (MFN2, GDAP-1) and those that play a role in axonal transport (DNM2) contribute mostly to axonal forms of CMT and are not discussed here in detail.

In summary, common molecular pathways provide rational targets for future therapeutic approaches aiming at larger groups of CMT patients.

1.2 Mouse models of CMT1A/ CMT1B/ CMT1X and the function of proteins mutated in these disorders

Besides the naturally occurring Tr and TrJ mutants (Suter et al., 1992a; Suter et al., 1992b), a series of mouse models have been generated for CMT; using mostly transgenic techniques (e.g.: PMP22tg mice, (Huxley et al., 1996) and homologous recombination (e.g.: P0 knockout mice, (Giese et al., 1992). These mutants provide essential knowledge about the biological function of molecules associated with CMT and the knowledge gained may pave the way towards diagnostic and therapeutic approaches in patients.

1.2.1. Peripheral myelin protein 22and animal models for CMT1A

Despite the fact that a 1.4 Mb duplication on chromosome 17 in the region carrying the *peripheral myelin protein 22 (PMP22)* gene accounts for the vast majority of CMT cases, our knowledge about the normal function of PMP22 is rather limited, especially when compared to that of other myelin proteins. PMP22 is a hydrophobic 22-kDa glycoprotein of 160 amino acids with four transmembrane domains. Its expression is regulated by two alternative promoters, with one being myelin-specific. PMP22 localizes almost exclusively to compact myelin, it builds 2–5% of the protein content of the myelin sheath and tends to oligomerize (Snipes et al., 1992; Tobler et al., 2002). Besides its structural role in myelin, PMP22 regulates cell spreading, migration, and apoptosis (Fabbretti et al., 1995; Brancolini et al., 1999; Brancolini et al., 2000; Sancho et al., 2001; Roux et al., 2005). Moreover, a recent study applying comparative expression profiling of mutant and wild-type sciatic nerves suggested that PMP22 has a role in the regulation of Schwann cell proliferation (Giambonini-Brugnoli et al., 2005).

Further knowledge about the function of PMP22 was provided by the several mutants generated. PMP22 knockout mice show a delayed onset of myelination and the formation of characteristic focal hypermyelinating structures (called tomacula). With aging tomacula disappear, and myelin and axonal degeneration occurs (Adlkofer et al., 1995). Thus, PMP22 is indispensable for myelination and myelin maintenance in peripheral nerves. Heterozygous PMP22-null mice revealed a milder phenotype and are a behaviorally and morphologically suitable model for HNPP (Adlkofer et al., 1997).

In the spontaneously occurring Tr and TrJ mutants (Suter et al., 1992a; Suter et al., 1992b) the primary structure of PMP22 is altered, which causes a disturbance of the intracellular protein folding and transport resulting in hypomyelination and increased Schwann cell numbers.

Transgenic animals carrying additional copies of the *PMP22* gene under the control of its own regulatory elements showed dose-dependent dysmyelinating and demyelinating neuropathies that reflect the more severe phenotype seen in occasional patients with four copies of *PMP22* (Reilly and Shy, 2009). As an example, homozygous transgenic rats with three extra copies of the murine *PMP22* gene developed severe demyelination; heterozygous rats were characterized by milder deficits, presenting with the impairment of motor abilities, slowed nerve conduction velocity and demyelination with onion bulb formation (Sereda et al., 1996). Additional *PMP22* mutants with 16 to 30 extra copies are severely affected due to the failure of myelin formation (Magyar et al., 1996). PMP22-overexpressing mice with seven copies of the human gene (C22) are characterized by a pronounced demyelination along with an obvious neuropathic phenotype. In contrast to this, heterozygous C61 mice with only four copies of *PMP22*, show a milder demyelination of the peripheral nerves (Huxley et al., 1996; Huxley et al., 1998). Heterozygous PMP22-overexpressing mice of the C61 strain backcrossed to C57/BL6 background (PMP22tg) were used in our experiments. In addition to the demyelinating hallmarks seen in the peripheral nerves and spinal roots, our laboratory described hypermyelinated fibers that increase in number with age (Kobsar et al., 2005).

1.2.2. Myelin protein zero and mouse models for CMT1B

Myelin protein zero (MPZ)/protein zero (P0) is expressed by Schwann cells and comprises about 50% of peripheral myelin protein. It is a transmembrane protein that consists of 219 amino acids and has a single transmembrane domain. Posttranslational modification occurs in the ER and Golgi apparatus including the addition of an *N*-linked oligosaccharide, sulfation, acylation, and phosphorylation (D'Urso et al., 1990). MPZ is a member of the immunoglobulin gene superfamily and functions as a homophilic adhesion molecule (Filbin et al., 1990). Crystallographic analysis of the extracellular domain demonstrated that it forms homotetramers interacting with each other in trans conformation (Shapiro et al., 1996). Studies describing several mutations in either the extracellular or the cytoplasmic domain of MPZ proved that both are necessary for homotypic adhesion (Warner et al., 1996; Filbin et al., 1999; Mandich et al., 1999). MPZ also has a regulatory role in myelination, which is probably a consequence of the MPZ-mediated signal transduction cascade (Xu et al., 2000; Menichella et al., 2001). Moreover, MPZ has also been suggested to interact with PMP22 to enforce adhesive interactions (D'Urso et al., 1999).

Absence of *MPZ* in knockout mice causes myelin to be uncompacted (Giese et al., 1992). Heterozygous knockout mice (P0+/-) that we used in our study show normal development until 10 weeks of age; however, at 4 months they develop a mild, but progressive neuropathy. Demyelination, remyelination with onion bulb formation and a reduced motor conduction velocity of around 30m/s are characteristics of the neuropathy seen in P0+/- mice (Martini et al., 1995). To date, there are more than 100 *MPZ* mutations known, most of which are missense. Accordingly, several mouse models were generated (e.g.: S63del, S63C, R98C). Based on the relatively mild phenotype of the heterozygous knockout mouse compared to the severe characteristics of point mutants, it was postulated that most *MPZ* mutations cause CMT by toxic gain-of-function or dominant negative effects rather than by pure loss of function (Berger et al., 2002). Of note, *MPZ* mutations cause dominant demyelinating, dominant axonal, and intermediate forms of CMT by various mechanisms.

1.2.3. Connexin32 and the connexin32 deficient mice as models for CMT1X

Mutations in the gap junction protein Cx32/GJB1 cause the X-chromosome linked CMT1X. Cx32 is expressed by many cell types including hepatocytes, oligodendrocytes, some neurons, and myelinating Schwann cells (Scherer et al., 1995). Despite the expression of Cx32 in such a large variety of tissues, peripheral neuropathy is generally the sole clinical manifestation of *GJB1* mutations, probably due to the compensatory effect of other connexins [reviewed in (Kleopa and Scherer, 2006)]. Cx32 is present in uncompact myelin, specifically in Schmidt-Lantermann incisures, paranodal loops, and at the internodal zone of partial myelin compaction (Meier et al., 2004). Connexin32 is highly conserved across mammalian species; it has a cytoplasmic carboxy and amino terminus and 4 transmembrane domains. Each connexon is a hexamer of connexin molecules forming a hemichannel that provides a contiguous pathway among the adjacent cells or cell compartments for diffusion of ions and other small molecules (<1kDa). It is assumed that Cx32 enables the communication between the abaxonal and adaxonal aspects of Schwann cell cytoplasm and the disruption of these radial pathways leads to demyelination via an unknown mechanism. *GJB1* mutations can be found both in the promoter and throughout the coding region of this gene, and as described above they result in a rather homogeneous phenotype.

In our investigations we used connexin 32 deficient mice (Cx32def) (Nelles et al., 1996) as a model for CMT1X. It is worth mentioning that several other models exist, including transgenic mice expressing 175fs, R142W, C280G, and S281X (reviewed in (Kleopa and Scherer, 2006). Cx32def mice serve as an authentic model for CMT1X and develop a progressive peripheral neuropathy starting at about 3 months of age with abnormalities comparable to those seen in patient biopsies. Characteristic features include abnormally thin myelin sheaths, cellular onion bulb formation reflecting de- and remyelination associated with Schwann cell proliferation; moreover, enlarged periaxonal collars and vacuole formation can be observed. Motor nerves are more severely affected than the sensory nerves, as also observed in P0 +/- mice. Neurophysiological examination revealed only slightly altered conduction properties (Anzini et al., 1997). Moreover, regenerating axonal clusters (Kobsar et al., 2003) and a maldistribution of potassium channels (Groh et al., 2010) could be observed.

1.3. The immune system as a mediator of pathology in genetic neuropathies

Several lines of evidence demonstrate that the immune system is involved in the pathogenesis of inherited demyelinating neuropathies. A substantial increase in CD8+ T cells and macrophages has been shown in the models of demyelinating CMT [reviewed in (Ip et al., 2006)] used in our studies (PMP22tg, P0+/-, Cx32def, together called 'myelin mutants'). The increase in the number of immune cells and the progression of the pathology occur in parallel and become more pronounced with aging. By crossbreeding P0+/- (Schmid et al., 2000) and Cx32def mice (Kobsar et al., 2003) with recombination activating gene (RAG)-1-deficient mutants that are lacking mature T- and B-lymphocytes, a marked alleviation of the demyelinating phenotype could be observed.

Macrophages contribute to the pathological alterations seen in inherited neuropathies. Myelin formation occurs normally in all mutants. But then macrophages enter the endoneurial tubes, phagocytose myelin and acquire a 'foamy' morphology due to the myelin debris they contain [reviewed in (Ip et al., 2006)]. Although such processes occur in all myelin mutants, important differences can be seen regarding myelin-macrophage association. In P0+/- and PMP22tg mice, macrophages phagocytose normal-appearing myelin, as they appear in direct contact with preserved myelin (Carenini et al., 2001; Kobsar et al., 2005). In contrast, in Cx32def mutants, macrophages are seen in contact with damaged or vacuolized myelin sheaths, suggesting they only invade structures that are already being degraded (Kobsar et al., 2002). The time course of macrophage number elevation also differs in the myelin mutants. Whereas P0+/- and Cx32def mice show gradually increasing macrophage numbers and morphological alterations, PMP22tg mice are characterized by high macrophage numbers and nerve damage already at 3 months of age, and remain relatively stable throughout the course of the disease. Sensory nerves of myelin mutants are preserved from degenerative changes (Martini et al., 1995; Shy et al., 1997); and interestingly, no elevation in macrophage numbers can be observed in them. Conceivably in sensory nerves there is either a lack of communication between Schwann cells and macrophages or naturally occurring macrophage inhibitors are present (Martini et al., 2008).

Two important mediators of macrophage survival and function are the Schwann cell derived chemokine ccl2 (also known as MCP-1: monocyte chemotactic protein-1) and the fibroblast derived CSF-1 (colony stimulating factor-1/ macrophage-CSF: M-CSF). These factors seem to play a complementary role in peripheral nerve pathology. Bone marrow transplantation studies strongly suggest that MCP-1 predominantly triggers the migration of macrophages to the diseased nerve (Fischer et al., 2008; Groh et al., 2010) and CSF-1 stimulates the proliferation of resident macrophages (Groh et al., 2012).

Beneficial effects of CSF-1 deficiency on myelin mutants have been documented (Carenini et al., 2001; Groh et al., 2012) by crossbreeding myelin mutants with osteopetrotic (op) mice that have an inactivating mutation in the coding region of CSF-1 (Yoshida et al., 1990). The latest study of our group on Cx32def mice described the rescue of the demyelinating phenotype, the preservation of axons and improved ion channel distribution and muscle innervation in the absence of CSF-1. This amelioration proved to be robust and persistent, lasting at least up to 12 months of age. In addition, this study identified endoneurial fibroblasts as the source of CSF-1 and confirmed that CSF-1 receptor (CSF-1R) is expressed on macrophages in peripheral nerves; setting common and well defined targets for potential therapeutic approaches (Groh et al., 2012).

The effects of CSF-1 are mediated through CSF-1R, a protein tyrosine kinase encoded by the c-*fms* proto-oncogene. It is a single pass transmembrane protein activated by ligand binding through oligomerization and trans-phosphorylation. IL34, a novel ligand of CSF-1R has recently been described (Lin et al., 2008).

1.4. Aim of the study

The above mentioned studies suggest that the inactivation of the CSF-1 pathway might be a highly promising treatment approach targeting a common, macrophage mediated pathway involved in the pathogenesis of several subtypes of CMT1. Therefore, we wished to analyze an orally-applicable, low molecular weight inhibitor of CSF-1R (CSF-1R inhibitor, CSF-1R specific kinase (c-FMS) inhibitor, PLX5622) as a candidate drug for treating three models for frequent forms of demyelinating CMT1 (CMT1A, CMT1B, CMT1X). The drug was applied following three different regimens corresponding to distinct scenarios described below, and mice were evaluated by a behavioral test, by neurophysiology and morphologically. Treated wild type and untreated mutant mice of the same age served as controls.

Treatment protocols:

1) Preventive approach:

Mice were treated from 3 months up to either 6 months or12 months of age.
Treatment was started before the onset of the increase in macrophage numbers and the parallel occurring demyelination and secondary axonal damage, in order to investigate whether CMT1A/CMT1B/CMT1X can be prevented or delayed by a short term (3 months) or long term (9 month) application of CSF-1R inhibitor.

2) Therapeutic approach:

CSF-1R inhibitor was administered from 9 months up to 15 months of age.
Mice already suffering from a full-blown disease were given the CSF-1R specific kinase inhibitor and analyzed whether treatment could stabilize or even improve the neuropathy, and possibly result in myelin and axon regeneration.

3) Reaction upon treatment interruption:

CSF-1R inhibitor was applied from 3 months up to 6 months of age and mice were evaluated at 12 months of age.
We wished to determine whether a rebound effect appears when treatment is terminated and drug is withdrawn (as seen in many anti-inflammatory protocols).

Protocols 1 and 2 are nearly completed, and animals have already been enrolled into protocol 3.

We expect that CSF-1R inhibitor would be an ideal candidate treatment being an orally-dosed inhibitor with limited or no side effects upon long-term application in a chronic disorder (according to Plexxikon Inc.). Based on observations of our group describing close macrophage-fibroblast contact in sural nerve biopsies of CMT1 patients (Groh et al., 2012); targeting the detrimental, low-grade inflammation would be highly relevant in subjects suffering from several forms of CMT1. In addition, PLX5622 has already been used in a phase I clinical trial for the treatment of rheumatoid arthritis (see Plexxikon Inc. website for further information). If CSF-1R inhibitor treatment proved beneficial, the latter two facts might allow a transition to clinical trials for patients with CMT1A/CMT1B/CMT1X and related peripheral neuropathies.

2. Material and Methods

2.1 Mutant mice and genotyping

Connexin32-deficient (Cx32def) (Nelles et al., 1996), P0 deficient (Giese et al., 1992) and transgenic (tg) PMP22-overexpressing mice of the C61 strain (Huxley et al., 1998) that were enrolled into the CSF-1R inhibitor treatment protocol had been backcrossed for more than 20 generations to a C57/BL6 background. Mice having the following genotypes: Cx32def, heterozygous P0 deficient (P0 +/-), heterozygous PMP22-overexpressing (PMP22tg), and wild type littermates (wt) were used for our investigations. Six mice per genotype per treatment protocol (see above) were enrolled into the study; however, not all of them have yet reached the desired age at the time point when the current work was written (see exact numbers at the individual experiments and in the figure legends). Cx32def mice being on a mixed C57BL/6 x 129Sv genetic background, were used as controls for preliminary electron microscopic evaluation (Groh et al., 2012) due to the temporary lack of genetic background matched controls. Genotypes were confirmed with conventional PCR reaction using DNA isolated from tail biopsies as described in detail (Schmid et al., 2000; Kobsar et al., 2003; Kohl et al., 2010a). Reaction conditions and primers are listed in the Appendix (7.1.4. and 7.1.5.). Briefly, genomic DNA was purified from tail biopsies using DNeasy blood & tissue kit from Qiagen (Hilden, Germany) according to the manufacturer's guidelines. PCR products were analyzed in 1% or 2% agarose gels in TBE buffer stained with ethidium bromide.

All mouse strains were kept in the animal facility of the Department of Neurology under barrier conditions and all experiments involving animals were approved by the local authority, the Regierung von Unterfranken (Project number: 55.2-2531.01 - 80/11)

.

2.2. CSF-1R inhibitor (PLX5622) treatment and determination of CSF-1 and PLX5622 levels

Rodent chow containing either 800 mg/kg or 1200 mg/kg CSF-1R specific kinase (c-FMS) inhibitor (PLX5622) was provided by Plexxikon Inc. Mice were being treated following treatment regimes mentioned in the aim of the study 1) from 3 months up to 6 months or 12 months of age, 2) from 9 months up to 15 months of age, 3) treated from 3 months up to 6 months of age and evaluated at 12 months of age (data incomplete when the current work is written and not further discussed). Moreover, a single mouse was treated from 3 month up to 6 months of age and sacrificed 24 hours after drug withdrawal. In addition, 5-6 month old animals were treated with PLX5622 for 14 days (3 wild types and 1 mutant per genotype for the 800 mg dosage and 3 wild types for the 1200 mg dosage).

To investigate whether drug concentrations reached the desired range and whether the treatment influenced CSF-1 levels; plasma, peripheral nerve, dorsal and ventral root, quadriceps muscle, brain, and liver tissue were harvested and sent for analysis to Plexxikon Inc. Plasma was collected after centrifuging heparinized blood gained by cardiac puncture in deep terminal anesthesia from untreated control and treated wild type and mutant animals. Tissue samples were quickly dissected and snap frozen in liquid nitrogen and sonificated in RIPA buffer. In addition, quadriceps muscle samples were homogenized before sonification. Mass spectrometry was applied to measure CSF-1R inhibitor concentration and CSF-1 levels were determined by ELISA according to previously established confidential protocols of Plexxikon Inc.

2.3. Equipment, reagents, solutions, buffers and antibodies

A detailed description of technical equipment (Appendix 7.1.1), reagents (Appendix 7.1.2), buffers and solutions (Appendix 7.1.3), PCR conditions and fragment sizes (Appendix 7.1.4.)

primer sequences (Appendix 7.1.5), as well as antibodies used for immunohistochemistry (Appendix 7.1.6) is provided in the Appendices.

2.4. Grip test

The strength of the hind limbs was evaluated using an automated Grip Strength Meter (Columbus Instruments, Columbus, OH, USA) as described previously (Fischer et al., 2008). Mice were trained to hold the grip bar, followed by the measurement of the peak force exerted by the mouse when pulled off the grip bar with a constant strength. Ten measurements per day were performed on three consecutive days and the average value of the measurements gained on the last day was used as outcome. Mice were weighed on the first day and animals of about the same weight were compared in the treated versus untreated groups. Female and male animals were analyzed separately.

2.5. Neurophysiological recordings

CSF-1R inhibitor treated mice and untreated littermates were anesthetized with 10µl/g body weight Ketamin-Rompun and placed under a heating lamp in order to maintain a constant body temperature (33-37°C) throughout the electrophysiological study (Neuro-MEP software). This technique has been described previously in detail (Zielasek et al., 1996). Briefly, supramaximal stimulation was performed at a distal (ankle, tibialis nerve) and a proximal (sciatic notch) site along the nerve using monopolar needle electrodes. Compound muscle action potentials (CMAP) were obtained with an active electrode inserted into the bulk of the paw muscles and a reference needle placed subcutaneously. Furthermore, sciatic nerve conduction velocity (NCV), H reflex and F-wave latency were recorded. All measurements were performed on the left side.
These experiments were carried out in collaboration with Dr. Wessig who was blinded to the genotype and treatment status of the mice.

2.6. Immunohistochemistry

Femoralis nerves and spinal roots for immunohistochemistry were dissected from mice that were deeply anesthetized and transcardially perfused with PBS for 5 minutes. Samples were either embedded in O.C.T. (Hartenstein, Wuerzburg, Germany) and cut into 10-µm-thick cross sections on a cryostat (Leica, Wetzlar, Germany), or the perineurium was stripped off and nerve fibers were loosely separated ("teased") and air dried.

Detailed information about the antibodies and the postfixation can be found in Appendix 7.1.6. In general, after postfixation the specimens were blocked with 5% BSA in PBS for 30 minutes followed by an overnight incubation with primary antibodies at 4°C. After washing three times with PBS, tissue samples were reacted with secondary antibodies at room temperature (45-60 minutes) and nuclei were stained with DAPI (Sigma-Aldrich, Taufkirchen, Germany). The specificity of the staining was controlled by omission of the primary antibodies. Fluorescence stainings were embedded in DABCO.

The quantification of endoneurial macrophages (rat anti-mouse F4/80 for macrophages; Serotec) and fibroblasts (rat anti-mouse CD34, eBioscience), and the assessment of the ratio of macrophages in contact with endoneurial fibroblasts, was performed on cross-sections according to previously published protocols (Carenini et al., 2001; Groh et al., 2012). For the latter, following avidin-biotin block, a biotinylated rat anti-mouse F4/80 (1:300, Serotec) primary antibody was applied and visualized by Cy3-conjugated Streptavidin (1:100, Biozol) (Groh et al., 2012). F4/80 is an extracellular antigen expressed on mature murine macrophages which is highly glycosylated and belongs to the subgroup of the G-protein-coupled receptor family, known as EGF-TM7.

The colocalization of CSF-1 Receptor (CSF-1R)(1:100, Santa Cruz) and the macrophage marker F4/80 was studied on teased fiber preparations (Groh et al., 2012). The integrity of the nodes of Ranvier was evaluated using a modification of a previously described protocol (Kohl et al., 2010a). Caspr1 (1:300, NIH, NeuroMab) labeled the paranodal region, and due to the

unavailability of Kv1.2. marker, Caspr2 (1:500, Millipore) was applied as a juxtaparanodal marker.

Light and fluorescence microscopic images were acquired using an Axiophot 2 microscope (Zeiss, Goettingen, Germany) equipped with a CCD camera (Visitron Systems, Tuchheim, Germany).

2.7. Ultrastructural analyses (semithin sections, electron microscopy)

Specimens of femoral nerves and lumbar ventral-and dorsal roots were processed for light and electron microscopy as described in detail elsewhere (Martini et al., 1995). Briefly, mice were anesthetized and perfused transcardially with PBS for three minutes followed by a 15 minute perfusion with 0.1 M cacodylate buffer, pH 7.4, containing 4% PFA and 2% glutaraldehyde. The tissue was subsequently postfixed overnight in the same buffer, osmificated with 2% osmiumtetroxide in 0.1 M cacodylate buffer for two hours at room temperature, dehydrated in ascending acetone concentrations and embedded in Spurr`s medium.

Semithin sections (0.5-µm-thick) were stained with alkaline methylene blue and analyzed by light microscopy (100 x magnifications). Ultrathin sections (100 nm) were transferred onto copper grids and stained with lead citrate. Analysis was performed using a ProScan Slow Scan CCD camera (Lagerlechfeld, Germany) mounted to a Leo 906 E electron microscope (Zeiss, Oberkochen, Germany) with a corresponding iTEM software (Olympus Soft Imaging Solutions GmbH, Münster, Germany).

2.8. Morphometric analyses

Pathological alterations were quantified applying multiple image alignment (MIA) that arranged vertically and horizontally overlapping electron microscopy images taken one after the other. It allowed a good quality overview of the whole nerve or spinal root cross section and made images

suitable for either a complete or a randomized analyses. Area measurements and manual tagging were performed on semithin sections using ImageJ software to determine the percentage of abnormally myelinated fibers, the percentage of macrophage – fibroblast contacts, and axon number per cross section. Axon diameter was measured by iTEM software on at least 100 axons/per animal in randomly selected fields of MIA images.

2.9 Statistical analyses

The investigator was blinded to the genotype and treatment status of the mice when performing quantification and morphometric analyses. Data is represented as mean value ± 1 standard error (SE). Statistical analysis was carried out using PASW Statistics 18 (SPSS, IBM) software. Sample data of macrophage and fibroblast counts, and grip test analysis were normally distributed and compared using One-Way ANOVA, followed by Tukey post hoc test or unpaired two-tailed Student's t-test when comparing CSF-1R inhibitor treated animals with untreated littermates. Statistical analyses of non-normally distributed neurophysiological and morphometric data was performed by the nonparametric Kruskal-Wallis test followed by Bonferroni correction when analyzing more than 2 groups and with Mann-Whitney U-test when comparing CSF-1R inhibitor treated versus untreated animals within the same genotype. Significance levels were labeled on figures as follows: * $p< 0.05$, ** $p< 0.01$, *** $p< 0.001$, and indicate relationship to wild type animals or untreated littermates of the same genotype as shown by the connecting markers.

3. Results

3.1. CSF-1 receptor as a target for the treatment of CMT

Our group previously demonstrated that CSF-1R is expressed on macrophages in the peripheral nervous system (Carenini et al., 2001; Groh et al., 2012). Being the target of our study, we wished to quantify the presence of CSF-1R on macrophages of wild type mice and the 3 different myelin mutants. Double immunohistochemistry on teased fiber preparations of the quadriceps nerve corroborated the colocalization of CSF-1R and the macrophage marker F4/80 **(Figure 3A)**. All CSF-1 positive profiles were also positive for F4/80 (data not shown) and about 90% of all macrophages expressed CSF-1R in 12 month old mice irrespective of the genotype **(Figure 3B)**. Thus, our results did not show a difference in the rate of CSF-1R positivity in macrophages of wild type or mutant quadriceps nerves. We only evaluated a limited number of younger animals from the Cx32def group and found that macrophages in 7 month old Cx32def mutants show a highly similar rate of positivity for CSF-1R to that of 12 month old animals **(Figure 3C)**.

Next, we investigated the plasma and tissue concentration of CSF-1R inhibitor (PLX5622). Mice (3 wild type and 1 mutant/per CMT model) were treated with 800-1200 mg drug/kg chow for 14 days which resulted invariably in a higher than 2 μM tissue concentration. According to Plexxikon Inc. the latter concentration leads to a strong reduction in Iba1, (ionized calcium binding adaptor molecule 1) which is specifically expressed on macrophages and is upregulated upon their activation. Mass spectrometry data is summarized in **Table 2**.

Table 2. CSF-1R inhibitor (PLX5622) concentrations.

Tissue	Plasma	Liver	Muscle	Brain	Spinal cord	Roots	Peripheral nerve
Concentration (μM) ± 1 SD	25.7 ± 6	60.3 ± 6.7	14 ± 3.6	14 ± 3.5	15.7 ± 4	17.7 ± 3.1	30.3 ± 11.6

Mass spectrometry data from mice treated with 1200 mg CSF-1R inhibitor/kg chow. Note that tissue concentrations are highly above 2 μM that is sufficient to reduce Iba1. Tissue concentrations in mice treated with 800 mg PLX5622/kg chow also exceeded this limit and were similar to those seen in mice treated with the higher dose (data not shown). The analysis was performed by Plexxikon Inc.

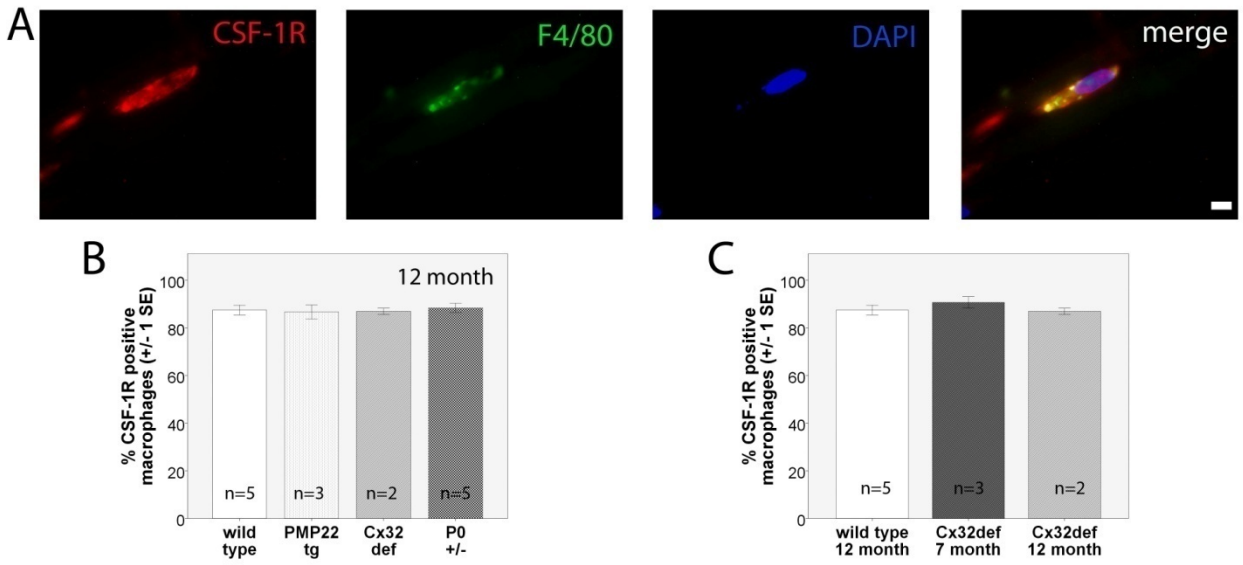

Figure 3.CSF-1R expression on macrophages. A) Double immunohistochemistry on teased fiber preparations of the quadriceps nerve confirming the colocalization of CSF-1R and the macrophage marker F4/80. Bar=10µm. **B-C)** Quantification of CSF-1R expression on macrophages. **B)** In wild type as well as in myelin mutant mice about 90% of all macrophages are positive for CSF-1R at 12 months of age. **C)** 7 month old Cx32def mutants show virtually the same rate of CSF-1R expression as 12 month old animals.

3.2. Reduction of macrophage numbers in the PNS of CSF-1R inhibitor treated wild type and myelin mutant mice, except for the quadriceps nerve of Cx32def mutants

We focused our attention on the analysis of the femoral quadriceps nerve (q.n.) and the ventral roots (v.r.), as the motor part of the PNS shows degenerative changes in myelin mutants occurring in parallel with the increase in macrophage numbers, while sensory nerves and dorsal roots seem to be almost completely preserved (Martini et al., 2008).

Five to six month old mice were treated with CSF-1R inhibitor for 14 days as mentioned above. By this age myelin mutants demonstrate a pronounced increase in macrophage numbers in the motor part of the PNS **(Figure 4 and 5)**. Already after the short period of treatment, macrophage numbers decreased in the quadriceps nerve of all animals. A marked difference was seen in wild type, PMP22tg and P0+/- mice with average macrophage numbers per cross section reduced to the 1-3 range, and a less pronounced decrease could be observed in Cx32def animals **(Figure 4C)**. These preliminary results gave a hint that the drug is exerting the expected effect; nevertheless, they need to be evaluated with caution as only a single mutant per genotype was analyzed.

We conducted a more extensive study in animals treated from 3 months up to 6 months of age. Consistent with the short term experiments, we found markedly decreased macrophage numbers both in the quadriceps nerve **(Figure 4A and B)** and the ventral roots **(Figure 5A and B)** of wild type (q.n. $p=0.022$; v.r. $p=0.037$), PMP22tg (q.n. $p<0.001$; v.r. $p=0.025$) and P0+/- mice (q.n. $p=0.014$;v.r. $p<0.001$). Surprisingly, we could not document a significant reduction in macrophage numbers in the quadriceps nerve of treated Cx32def mutants **(Figure 4A and B),** which is in contrast with the findings of short term treatment. However, there was a marked reduction in macrophage numbers in the ventral roots of these animals ($p=0.002$) when compared to untreated littermates **(Figure 5A and B)**. Moreover, we observed a pronounced increase in the area of the quadriceps nerve cross section in treated Cx32def mice **(Figure 4A)**.

Preliminary data from PMP22tg mice treated from 9 months up to 15 months of age suggested that CSF-1R inhibitor treatment decreased macrophage numbers in the quadriceps nerve even in this late, full blown stage of the disease **(Figure 4D)**. Having a single 15 month old untreated PMP22tg control mouse limits the value of this preliminary observation. Nevertheless, it is worth noting that macrophage numbers in PMP22tg mice treated from 9 months up to 15 months of age are strongly reduced when compared to untreated 6 month old (14.02 macrophages/ cross section, n=6) or 12 month old PMP22tg animals (Kohl et al., 2010b).

Taken together, CSF-1R inhibitor proved to be efficient in reducing the macrophage numbers persistently in at least two distinct mouse models of CMT1.

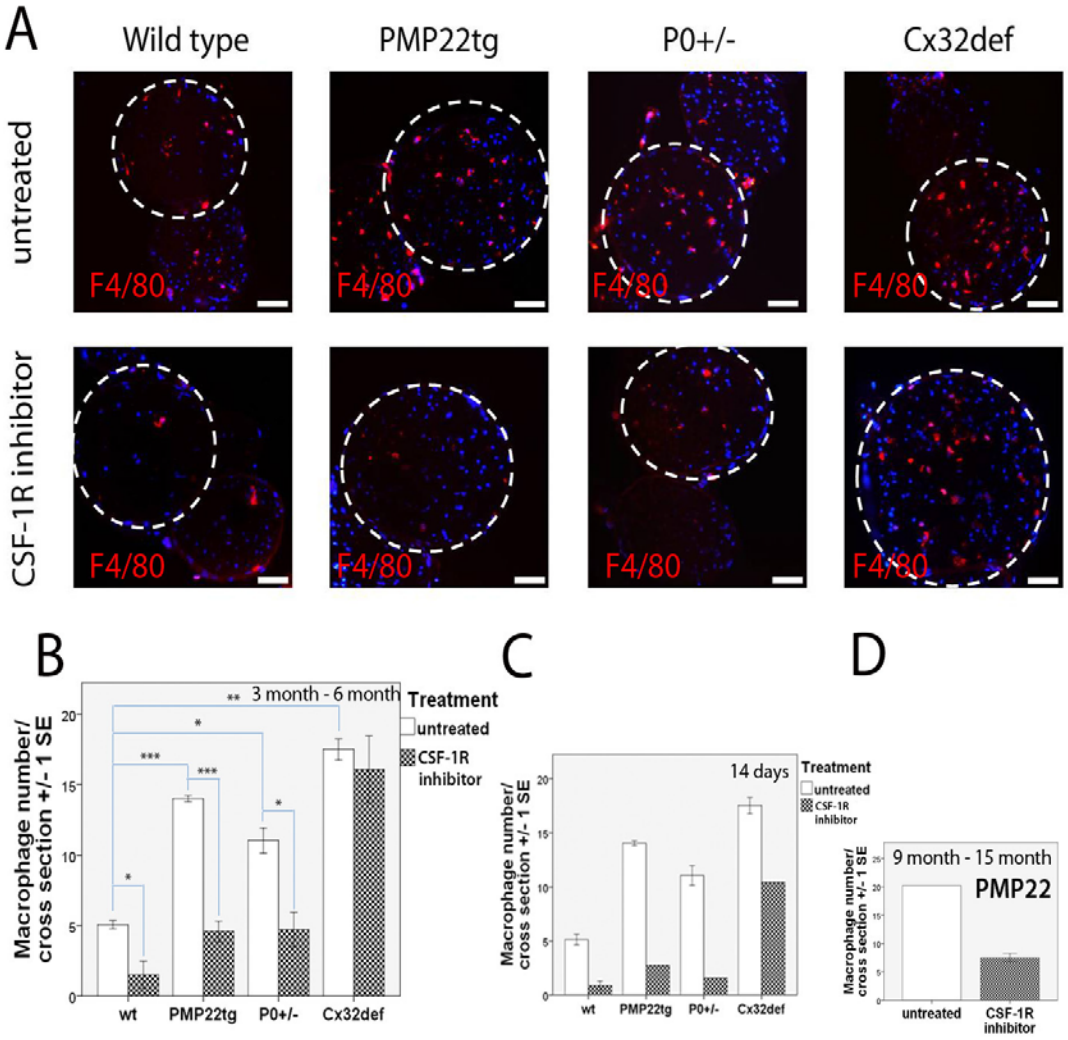

Figure 4. Macrophage numbers in the quadriceps nerve of CSF-1R inhibitor treated and untreated mice. A) Immunohistochemistry against the macrophage marker F4/80 on quadriceps nerve cross sections of 6 month old control and treated (from 3 months up to 6 months of age) mice. Note the dramatic reduction in the number of F4/80 positive profiles in CSF-1R inhibitor treated wt, PMP22tg and P0+/- mice, but not in Cx32def mutants. Bar=50µm. **B-D)** Quantification of macrophage numbers in the quadriceps nerve. **B)** CSF-1R inhibitor treatment from 3 months up to 6 months of age. Compared to wild type littermates, macrophage numbers were significantly increased in untreated PMP22tg ($p<0.001$), P0+/- ($p=0.001$) and Cx32def mice ($p<0.001$). CSF-1R inhibitor treatment resulted in a significant reduction of macrophage numbers in wt ($p=0.022$), PMP22tg ($p<0.001$) and P0+/- mice ($p=0.014$), but not in Cx32def mutants. n=3/genotype/treatment group. **C)** Fourteen days of CSF-1R inhibitor treatment lead to a marked reduction of F4/80 positive profiles in the quadriceps nerve. n=1-3. **D)** Macrophage numbers decreased in the quadriceps nerve of PMP22tg mice treated with CSF-1R inhibitor from 9 months up to 15 months of age (n=3) compared to an untreated animal n=1.

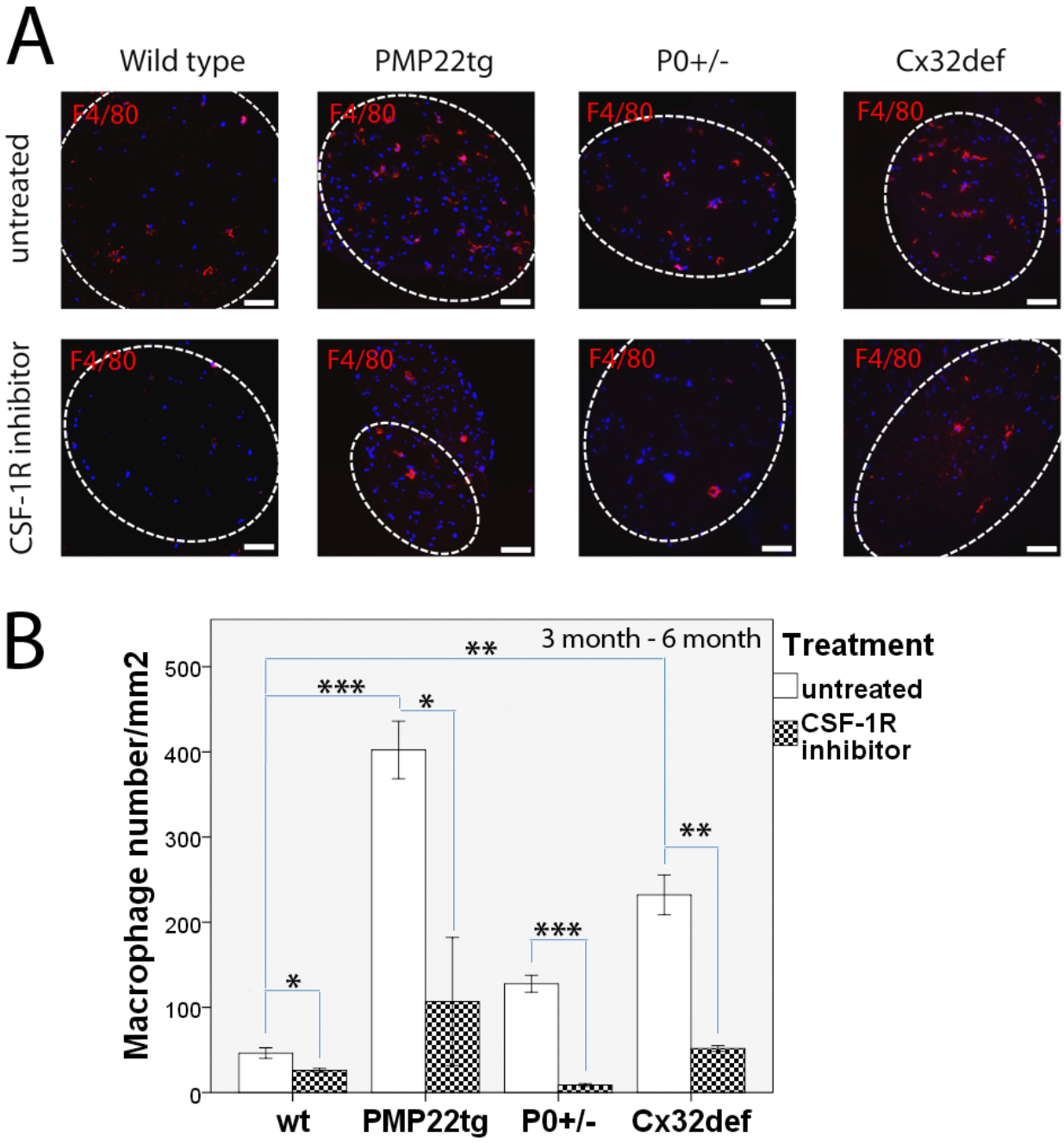

Figure 5. Macrophage numbers in the ventral roots of CSF-1R inhibitor treated and untreated mice. A) Immunohistochemistry against F4/80 on ventral root cross sections indicated a reduction of macrophage numbers in all CSF-1R inhibitor treated mice. Bar=50µm. **B)** Quantification of F4/80 positive profiles in the ventral roots. Note the pronounced upregulation of macrophage numbers in myelin mutants compared to wild type mice (PMP22tg $p<0.001$; Cx32defp=0.001). CSF-1R inhibitor treatment resulted in a significantly lower macrophage number both in wild type and myelin mutant mice (wt $p=0.037$; PMP22tg $p=0.025$; P0+/- $p<0.001$; Cx32def $p=0.002$). n=3/genotype/treatment group.

3.3. Alteration of CSF-1 concentration

After having shown the effect of PLX5622 on macrophages, we determined whether the blockage of CSF-1R altered the CSF-1 levels. Indeed, CSF-1 plasma and tissue levels, detected by ELISA were significantly elevated in the CSF-1R inhibitor treated animals **(Table 3)**, suggesting that fibroblasts upregulated their CSF-1 production.

Table 3. CSF-1 concentrations.

CSF-1 Concentration (pg/ml) ± 1 SD	Control	CSF-1R inhibitor treated
Plasma	384 ± 301	659 ± 321
Liver	58	402 ± 11
Muscle	blank	194 ± 95
Brain	163	379 ± 46
Spinal cord	82	677 ± 97
Root	60	224 ± 10
Peripheral nerve	76	284 ± 79

ELISA data from mice treated with 1200 mg CSF-1R inhibitor/kg chow. CSF-1 plasma and tissue concentrations of CSF-1R inhibitor treated mice were higher than those of untreated littermates. CSF-1concentrations in mice treated with 800 mg PLX5622/kg chow were also markedly elevated compared to untreated values (data not shown). The analysis was carried out by Plexxikon Inc.

3.4. Potential rebound effect upon withdrawal of PLX5622

Having recognized the upregulation of CSF-1, we considered the possibility of a rebound effect upon the withdrawal of CSF-1R inhibitor. We gained preliminary data from a 6 month old PMP22tg mouse that was treated from 3 months up to 6 months of age and had been off the drug for 24 hours before being sacrificed. We experienced a dramatic upregulation of macrophage numbers not only in the quadriceps nerve **(Figure 6A and C)**, but also in the saphenus nerve (**Figure 6A** – not circled tissue; 16.6 macrophage/cross section versus 4-5 macrophages/cross section in untreated PMP22tg mice) which is only very mildly affected in untreated PMP22tg

mice. In addition, macrophage numbers were upregulated in the ventral roots **(Figure 6 B and D)**. Macrophage numbers in both the femoralis nerve and the ventral root exceeded the number observed before the administration of CSF-1R inhibitor. These data suggest the presence of a strong rebound effect; however, more animals need to be included, and the duration of rebound effect and the long term morphological consequences need to be evaluated carefully.

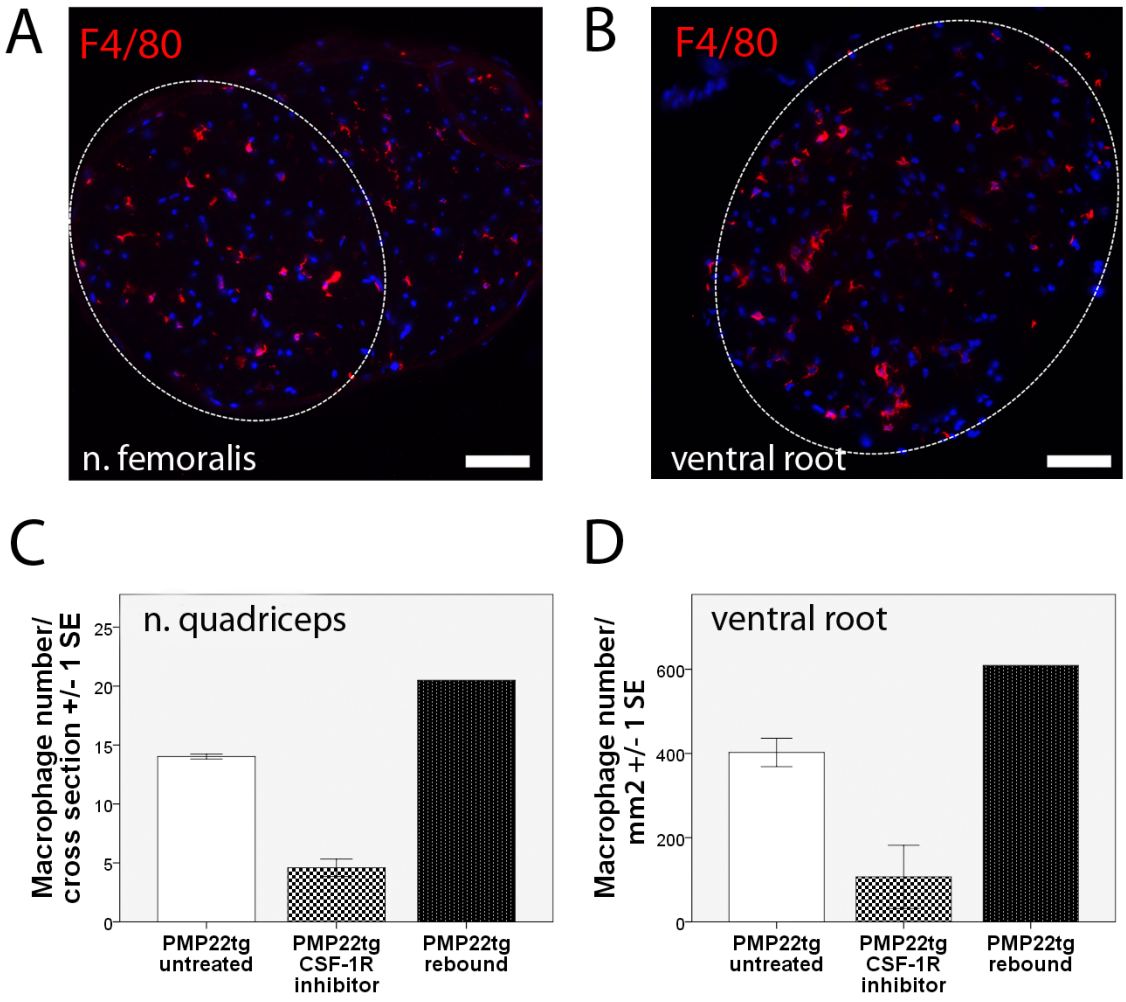

Figure 6. Elevation of macrophage numbers after the termination of CSF-1R inhibitor treatment.
A) and B) F4/80 immunohistochemistry on **A)** femoralis nerve (with the quadriceps nerve circled) and **B)** ventral root cross sections of a 6 month old PMP22tg mouse whose treatment was stopped 24 hours before being sacrificed. Bar=50µm. **C) and D)** Quantification of F4/80 positive profiles in **C)** the quadriceps nerve and **D)** the ventral root revealed a higher macrophage number after the termination of treatment than was observed before the application of PLX5622. PMP22tg rebound n=1, PMP22tg untreated and CSF-1R inhibitor n=3.

3.5. The effects of CSF-1R inhibitor treatment on fibroblasts

Endoneurial fibroblast are the source of CSF-1 in the PNS (Groh et al., 2012) and are known to be upregulated in number in all of the myelin mutants studied **(Figure 7A and B)** compared to wild type mice (PMP22tg p=0.009, Cx32def p=0.007). Again, we studied the three different age groups (treated for 14 days, treated from 3 months up to 6 months of age or from 9 months up to 15 months of age). In spite of the elevation of CSF-1 levels, we found no significant change in fibroblast numbers between untreated and CSF-1R inhibitor treated animals within the same genotype in any of the above mentioned age groups **(Figure 7A-D)**.

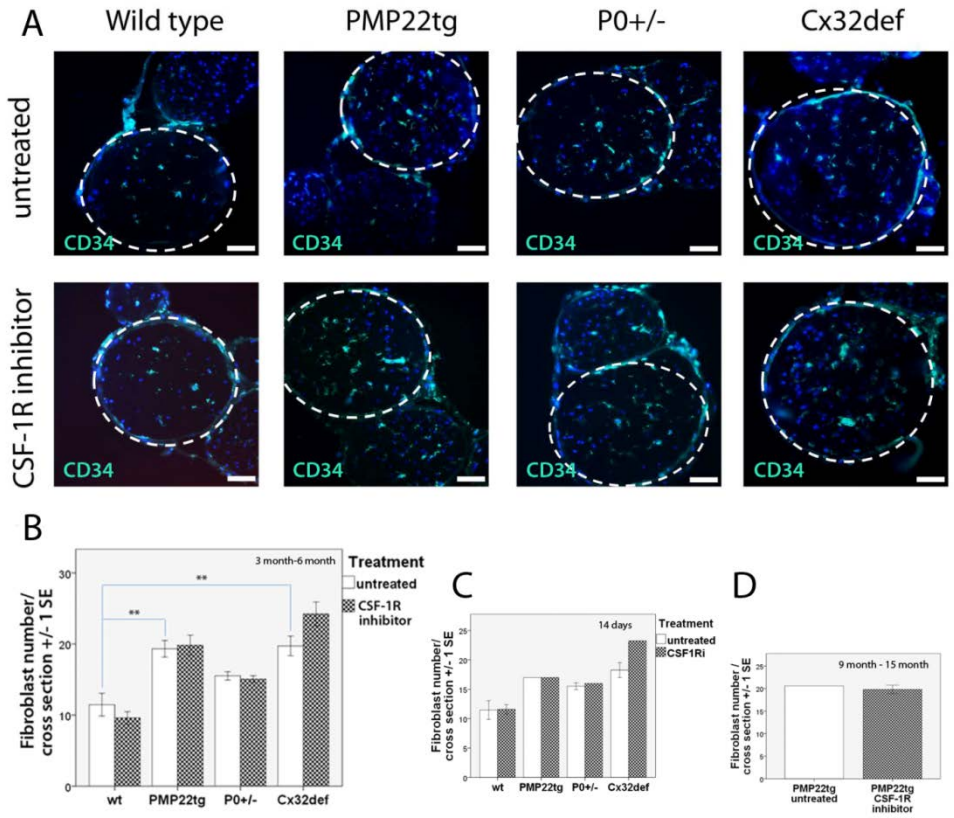

Figure 7. Fibroblast numbers in the quadriceps nerve of CSF-1R inhibitor treated and untreated mice. A) Immunohistochemistry against the fibroblast marker, CD34 on quadriceps nerve cross sections. Bar=50µm **B-D)** Quantification of fibroblast numbers in the quadriceps nerve of untreated and CSF-1R inhibitor treated mice. **B)** CSF-1R inhibitor treatment from 3 months up to 6 months of age. Note the higher number of fibroblasts in myelin mutant mice (PMP22tg p=0.009; Cx32def p=0.007). CSF-1R inhibitor treatment did not alter fibroblast numbers. n=3/genotype/treatment group. **C)** 14 days of CSF-1 R inhibitor treatment (n=1-3/genotype/treatment group) **D)** or treatment of PMP22tg mice from 9 months up to 15 months of age did not affect fibroblast numbers either. n=1-3/treatment group.

About 60% of macrophages in both wild type and myelin mutant mice are known to be in contact with fibroblasts (Groh et al., 2012). The CSF-1 R probably provides the base of contact between these two cell types, so we investigated whether inhibition of the CSF1R kinase altered this close relationship. Indeed, we found that a higher percentage (70%-100%) of macrophages were in contact with a fibroblast in CSF-1R inhibitor treated animals **(Figure 8)**. This phenomenon underlines the importance of CSF1 for the survival of macrophages and also suggests that only macrophages that remain in contact with fibroblasts - and thus are still stimulated in spite of the treatment with PLX5622 - survive.

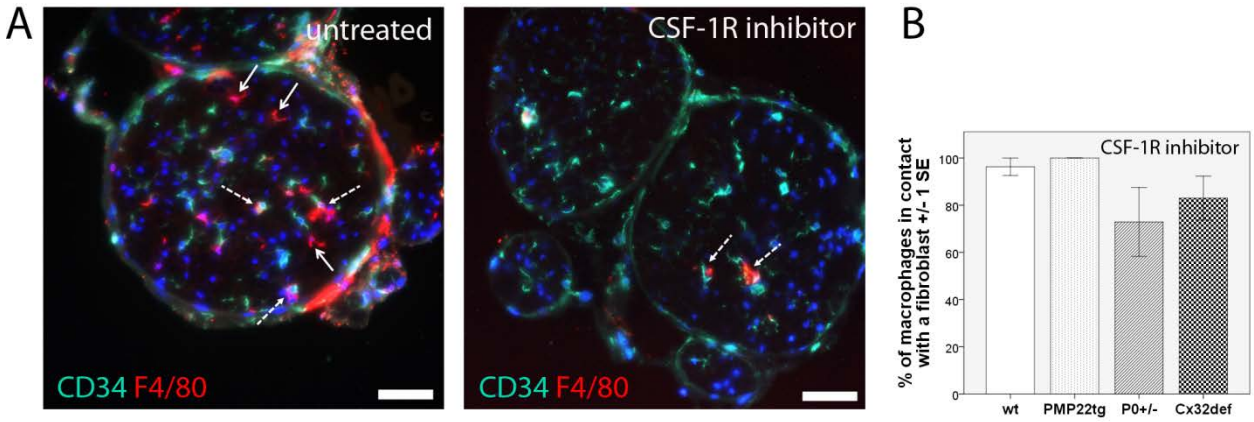

Figure 8.Macrophage-fibroblast contact in CSF-1R inhibitor treated and untreated mice.
A) Double immunohistochemistry against CD34 and F4/80 on cross sections on quadriceps nerves of untreated and CSF-1R inhibitor treated PMP22tg mice. Dashed arrow: macrophages in contact with fibroblasts, solid arrow: macrophages not in contact with fibroblasts. Bar=50µm. **B)** Quantification of macrophage – fibroblast contact in CSF-1R inhibitor treated wild-type and mutant mice. Higher association rates were observed in CSF-1R inhibitor treated animals of each strain; untreated littermates had about 60% association rate (data not shown). n=3/genotype.

3.6. Behavioral and neurophysiological analysis of wild type and myelin mutant mice treated with CSF-1R inhibitor from 3 months up to 6 months of age

In order to explore the functional consequences of the reduction in macrophage numbers, mice treated with CSF-1R inhibitor from 3 months up to 6 months of age and control littermates underwent grip test analysis and neurophysiological examination.

The peak force exerted on grip test was studied separately in female and male mice and revealed no significant differences in CSF-1R inhibitor treated versus untreated animals. It is worth mentioning that PMP22tg and Cx32def mice showed a tendency to perform worse than wild type animals and this performance even deteriorated in CSF-1R inhibitor treated male PMP22tg mice **(Figure 9)**.

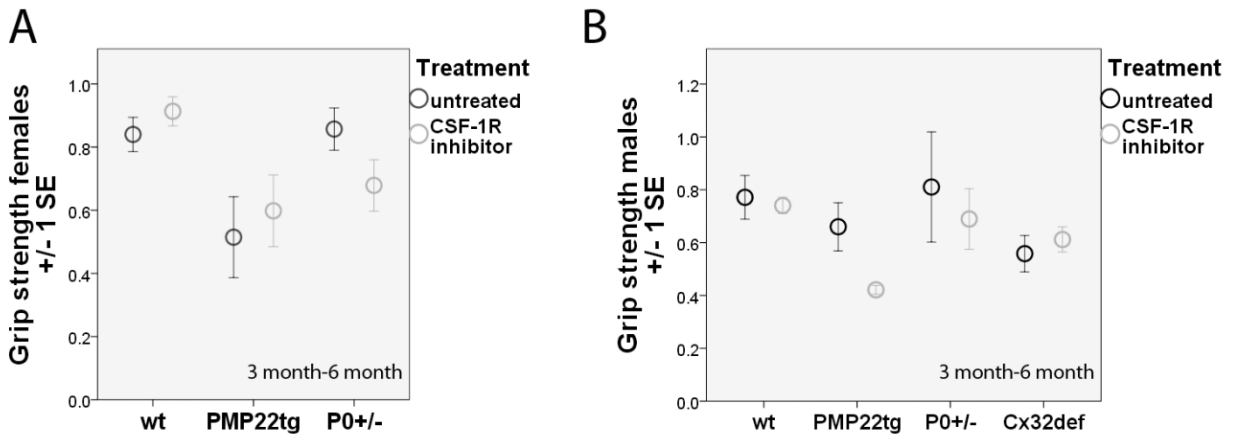

Figure 9.Measurement of grip strength in CSF-1R inhibitor treated (from 3 months up to 6 months of age) and untreated mice.

A) and B) Peak force exerted on grip strength analysis in **A)** female and **B)** male CSF-1R inhibitor treated mice (from 3 months up to 6 months of age) compared to untreated littermates. Differences in the performance did not reach significance, but untreated PMP22tg and Cx32def mice showed a tendency to be weaker than wild type animals. CSF-1R inhibitor treatment did not result in an improvement in muscle strength. n=2-4.

Cx32def mice when crossbred with osteopetrotic(op) mice (that harbor an inactivating mutation in the coding region of the CSF-1 gene) presented with a persistent and robust amelioration of demyelination and axonopathic changes, and had preserved neuromuscular junctions (Groh et al., 2012). Due to considerably smaller size of these animals neurophysiological measurements could not be performed to study the functional consequences of the morphological amelioration. Therefore, our aim was to investigate whether the pharmacological blockade of CSF-1 would lead to alterations in neurophysiological parameters.

Unexpectedly, we documented a consequent decrease of CMAP amplitudes gained by both distal and proximal stimulation in all groups examined **(Table 4)**. The already reduced CMAP amplitudes of myelin mutants (PMP22tg dist CMAP p=0.008; prox CMAP p=0.013) were further diminished by CSF-1R inhibitor treatment (P0+/- dist CMAP p=0.009, P0+/- prox CMAP p=0.008; Cx32def dist CMAP p=0.037), referring rather to axonal damage than to the amelioration of the phenotype **(Figure 10)**. CSF-1R inhibitor treatment of wild type mice lead not only to a significant decrease in CMAP amplitudes (dist CMAP p=0.041; prox CMAP p=0.084) but also to a reduction in the nerve conduction velocity (p=0.04; **Figure 10**) reflecting either a potential damage of the myelin sheath or other structures that influence saltatory conduction (ion channels, internodal length, etc.).

In addition, H reflex and F wave parameters were examined to evaluate the extent that proximal segments of the PNS, including the spinal roots, were affected. H reflex and F wave latencies were only slightly prolonged in P0+/- and Cx32def animals, but were markedly delayed in PMP22tg animals (p=0.02; **Table 4**). Three months of CSF-1R inhibitor treatment altered neither H reflex nor F wave latencies **(Table 4)**. Thus, treatment did not correct the myelination defects of proximal PNS segments.

Table 4. Neurophysiological parameters of CSF-1R inhibitor treated (from 3 months up to 6 months of age) and untreated wild type and myelin mutant mice. Significant differences caused by the treatment are marked in red and analyzed in Figure 10.

genotype	treatment	dist lat (ms)	dist dur (ms)	dist ampl (mV)	prox lat (ms)	prox dur (ms)	prox ampl (mV)	d(mm)	NCV (m/s)	n
wild type	0	0.81	2.3	14.8	1.29	2.2	11.7	21	43.9	8
wild type	CSF-1R inhibitor	0.87	3.0	10.0	1.49	2.7	7.6	21	34.0	6
PMP22 tg	0	1.29	3.1	7.3	2.08	3.0	6.0	21	27.9	7
PMP22 tg	CSF-1R inhibitor	1.39	3.6	7.0	2.20	4.1	4.5	21	26.7	5
P0 +/-	0	1.06	2.8	13.0	1.83	2.3	8.2	23	29.6	3
P0 +/-	CSF-1R inhibitor	1.03	3.0	7.1	1.76	3.0	4.4	21	29.3	6
Cx32def	0	0.96	3.3	13.5	1.71	2.7	10.2	21	28.3	9
Cx32def	CSF-1R inhibitor	0.87	2.7	9.4	1.53	2.3	7.2	22	33.5	6

genotype	treatment	H lat (ms)	F lat (ms)	H pers (%)	F pers (%)	n
wild type	0	4.7	4.4	13	100	8
wild type	CSF-1R inhibitor	4.5	4.7	34	100	6
PMP22 tg	0	6.9	7.1	10	100	7
PMP22 tg	CSF-1R inhibitor	7.2	7.6	10	98	5
P0 +/-	0	4.9	4.9	10	100	3
P0 +/-	CSF-1R inhibitor	5.3	5.6	15	100	6
Cx32def	0	5.0	5.2	12	100	9
Cx32def	CSF-1R inhibitor	4.5	4.9	53	97	6

dist: distal, prox: proximal, lat: latency, dur: duration, ampl: CMAP amplitude, d: distance, H: H reflex, F: F wave, pers: persistence, ms: millisecond, mV: millivolt, mm: millimeter

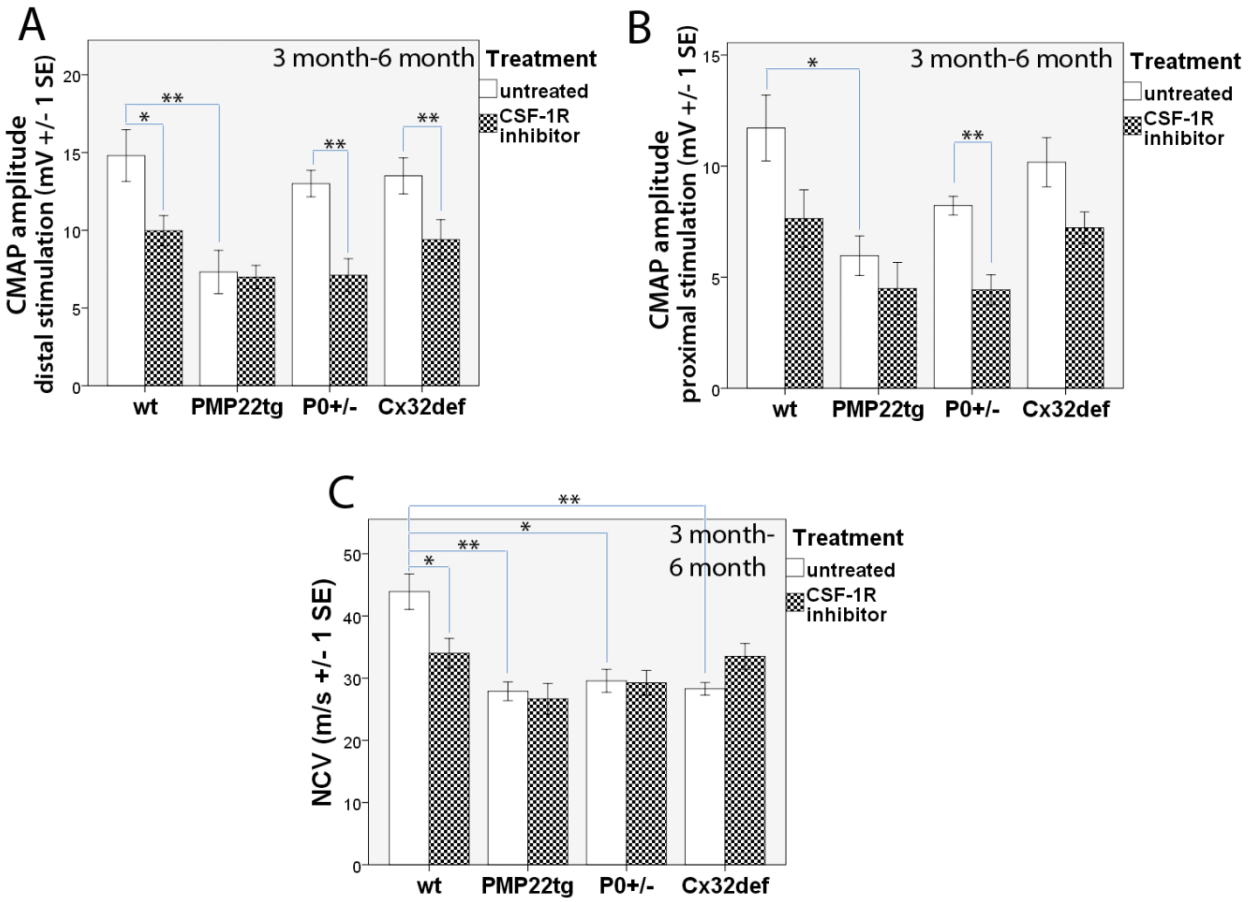

Figure 10. Deterioration of neurophysiological parameters in mice treated with CSF-1R inhibitor from 3 months up to 6 months of age.

A) and B) Compound muscle action potentials of myelin mutant mice were reduced compared to those of wild type littermates (PMP22tg dist CMAP p=0.008; prox CMAP p=0.013) and decreased further with CSF-1R inhibitor treatment as measured by A) distal (P0+/- p=0.009, Cx32def p=0.037) and B) proximal stimulation (P0+/- p=0.008). In addition, CSF-1R inhibitor treated wild type mice presented with significantly lower CMAP amplitudes than untreated animals (distal stimulation p=0.0041). n=3-9. C) Myelin mutants were characterized by reduced nerve conduction velocities (30 m/s range) (PMP22tg p=0.001; P0+/- p=0.014; Cx32def p=0.001) that remained unaffected by CSF-1R inhibitor treatment. In wild type mice treatment resulted in significantly diminished conduction velocities (p=0.04). n=3-9.

3.7. Morphological alterations in mice treated with CSF-1 R inhibitor from 3 months up to 6 months of age

Our group previously demonstrated that the lack of CSF-1 resulted in a prominent improvement of the morphological phenotype in P0 +/- (Carenini et al., 2001) and Cx32def mice (Groh et al., 2012); moreover, unpublished data (Groh J, Martini R) suggested a similar benefit in PMP22tg mice. Unexpectedly, the blockage of CSF-1R did not lead to such uniform positive changes regarding the morphological phenotype of myelin mutant mice.

Abnormally myelinated axons - including hypermyelinated profiles in PMP22tg mice and hypo- or demyelinated axons in all 3 myelin mutants - were still present both in the quadriceps nerve and the ventral roots even after 3 months of CSF-1R inhibitor treatment **(Figure 11 and 12)**. The percentage of abnormally myelinated fibers remained practically the same in PMP22tg, Cx32def mutants and in the quadriceps nerve of P0+/- mice **(Figure 13)**. These morphological data are in line with the electrophysiological findings, namely the unchanged NCVs, H-reflex and F wave latencies. By contrast, we documented a significant increase in the percentage of normally myelinated fibers ($p=0.03$) and in parallel a decrease in the percentage of thinly- ($p=0.052$) or demyelinated fibers ($p=0.003$) in the ventral roots of treated P0+/- mice **(Figure 13B)**, reflecting a beneficial effect of the reduction in macrophage numbers due to CSF-1R inhibitor treatment.

Foamy macrophages, loaded with myelin debris **(Figure 11B and 12B)** were present in both the quadriceps nerve and ventral roots of CSF-1R inhibitor treated P0+/- and Cx32def mice and in the ventral roots of PMP22tg mutants **(Figure 13D)**, but could not be detected in untreated or treated wild type mice. The number of foamy macrophages was similar in untreated and treated mutants, except for the quadriceps nerve of Cx32def mice, where a marked reduction could be noted **(Figure 13D)**. The latter needs to be evaluated with caution because control animals were on a mixed background (see above), and because this is the only PNS tissue where the overall macrophage number was not lowered by CSF-1R inhibitor treatment. These results indicate that actively phagocytosing macrophages did not completely disappear upon the blockage of CSF-1R in myelin mutants.

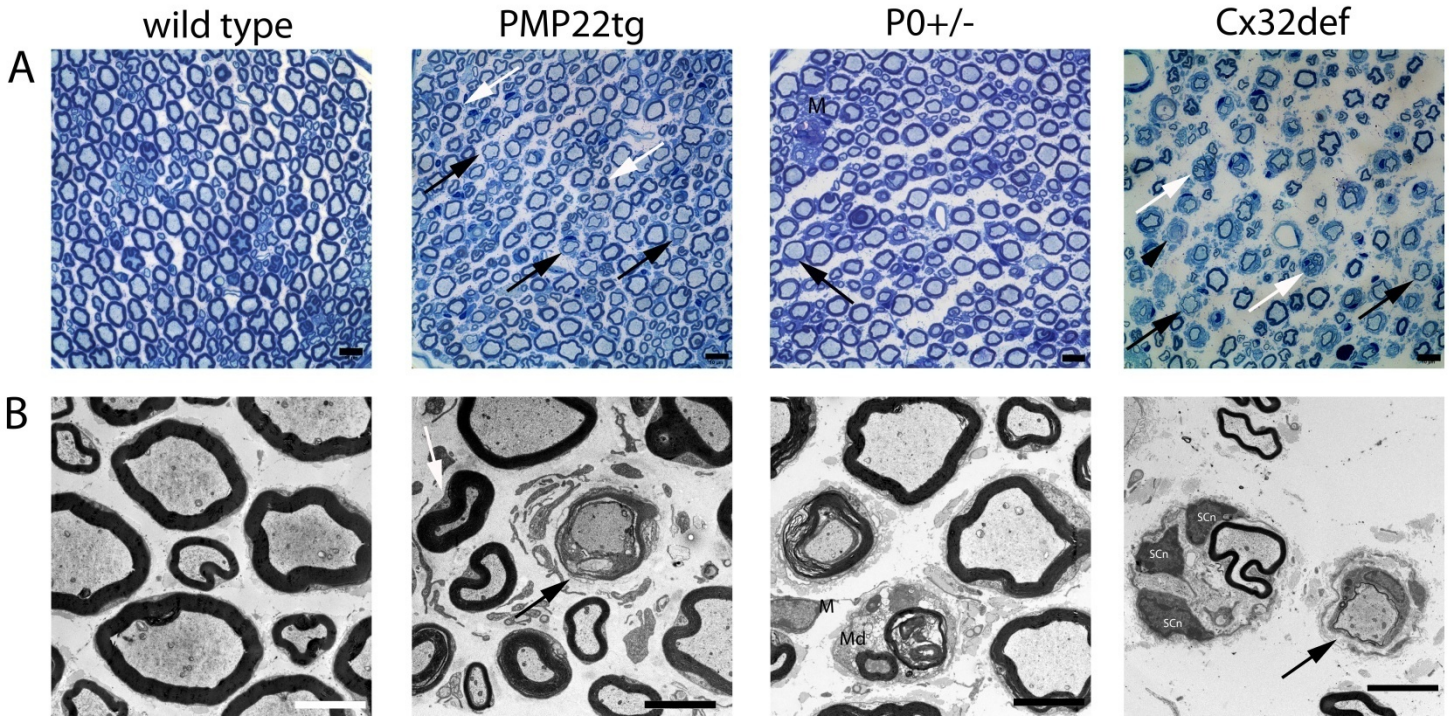

Figure 11.Morphological characteristics of the quadriceps nerve of CSF-1R inhibitor treated (from 3 months up to 6 months of age) mice.

A) light microscopic images of semithin and **B)** electron microscopic images of ultrathin quadriceps nerve cross sections from CSF-1R inhibitor treated mice. Wild type mice showed normal myelin and axonal characteristics. Images of myelin mutant nerves replicated the typical pathological findings observed in untreated mutants. PMP22tg mice were characterized by the presence of both hypo- (black arrows) and hypermyelinated (white arrows) fibers. A limited number of thinly myelinated axons could be seen in P0+/- mice (black arrows); moreover, actively phagocytosing macrophages (M; Md: myelin debris) were present in the treated animals. Cx32def mice presented with prominent pathological alterations, such as thinly myelinated fibers (black arrows), regeneration clusters (white arrows) and onion bulb formation (arrowhead). The electron microscopic image illustrates 3 Schwann cell nuclei (Scn) surrounding one fiber, which might signal the onset of onion bulb formation. **A)** Bar=10 μM **B)** Bar=5 μM

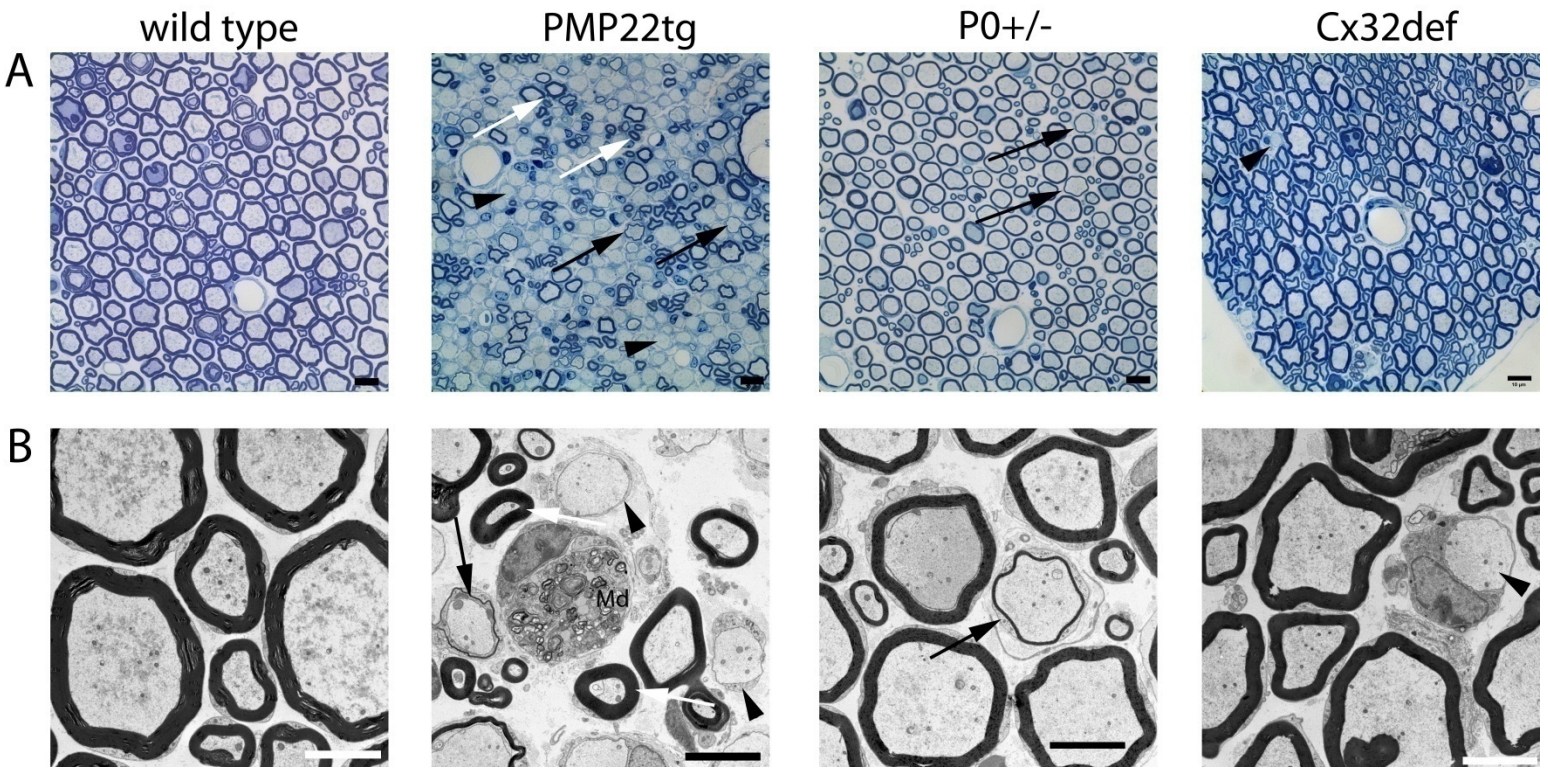

Figure 12. Ventral root pathomorphology in myelin mutants treated with CSF-1R inhibitor from 3 months up to 6 months of age. Representative **A)** light microscopic semithin and **B**) electron microscopic ultrathin sections of lumbar ventral roots of wild type and myelin mutant mice treated with CSF-1R inhibitor from 3 months up to 6 months of age. Wild type animals show normal myelination and no obvious sign of axonal pathology. Besides a considerable number of thinly- (black arrows) or demyelinated (arrowheads) axons hypermyelinated fibers (white arrows) remained detectable in treated PMP22tg mice. A low number of abnormally myelinated axons (thinly myelinated: black arrows, demyelinated: arrowheads) could also be observed in P0+/- and Cx32 def mice. **A)** Bar=10 µM **B)** Bar=5 µM

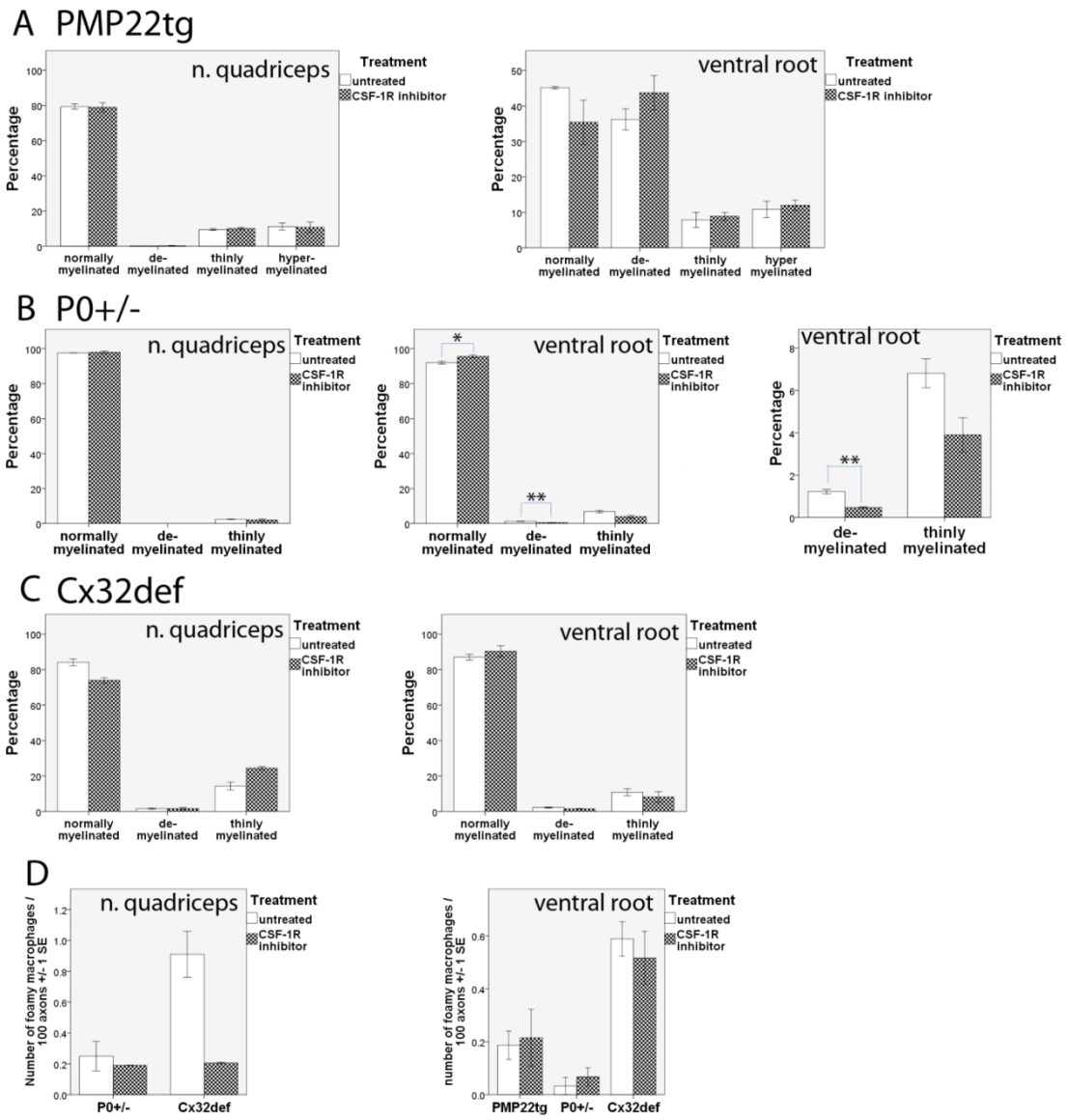

Figure 13. Myelination state of the quadriceps nerve and the lumbar ventral roots in CSF-1R inhibitor treated mice.

A) - C) Distribution of normally/abnormally myelinated fibers in the quadriceps nerve and ventral roots of myelin mutant mice. No improvement could be documented in treated PMP22tg and Cx32def mice. However, the ventral roots of CSF-1R inhibitor treated P0+/- mice revealed a significantly higher number of normally myelinated fibers (p=0.03) in parallel with a decrease in the number of de-/hypomyelinated fibers (see higher magnification graph to the right; p=0.003 and p=0.0052 respectively). **D)** Foamy macrophages, identified by electron microscopy were still present in all of the treated mutants. Preliminary data suggests a decrease in the number of foamy macrophages in the quadriceps nerve of treated Cx32def animals, but not in P0+/- quadriceps nerves or in the ventral roots of myelin mutants.

Next, we investigated the axonal characteristics of myelin mutants searching for possible deficits that might explain the decrease in CMAP amplitudes. Wild type animals did not show any direct sign of axonal pathology (vacuoles, enlarged periaxonal collars, etc.; **Figure 11 and 12**); furthermore, we observed no difference in the distribution of axon diameter (Figure 13A) and the overall number of axons in the quadriceps nerves **(Figure 14B)** between treated and untreated animals. The same held true for the axonal characteristics of PMP22tg mice. In contrast, we noticed that the axon diameter distribution was shifted to the left, towards small caliber axons in both P0+/- and Cx32def mice **(Figure 14A)**. The percentage of large caliber fibers was markedly reduced, axons larger than 7 μm in diameter were virtually missing or represented a minor part of axons compared to untreated mice. Accordingly, the average axon diameter was also significantly reduced in P0+/- and Cx32def mice ($p<0.001$ for both). In addition the overall axon number was slightly, but significantly reduced in both P0+/- ($p=0.002$) and Cx32def ($n=2$ in the treated group did not allow to carry out statistical analyses) mutants **(Figure 14B)**.

Regeneration clusters, typical hallmarks of the Cx32def neuropathy **(Figure 11)** appeared much more frequently in CSF-1R inhibitor treated mice than in untreated littermates **(Figure 14C)**. Again, we could not exclude that this difference is due to the slightly different genetic background.

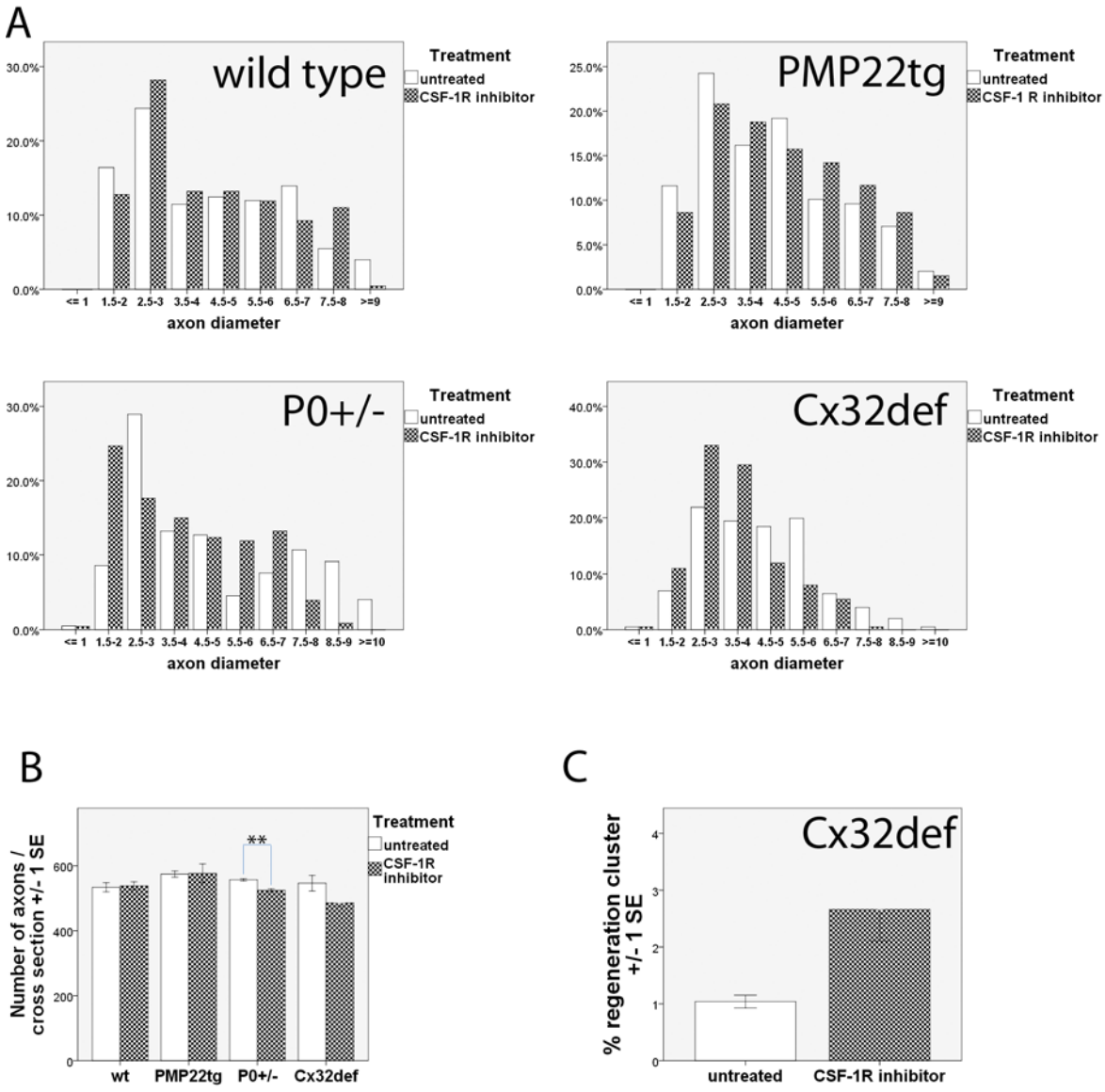

Figure 14. The effect of CSF-1 R inhibitor treatment on axonal properties of the quadriceps nerve.

A) Distribution of axon diameter. CSF-1R inhibitor treatment did not significantly influence the distribution of axon diameter in wild type and PMP22tg mice. In contrast, note the decrease in the percentage of large diameter axons in treated P0+/- and Cx32def mutants. n=2/ genotype/treatment group. **B)** Number of axons in the quadriceps nerve. A lower overall axon number could be detected in CSF-1R inhibitor treated P0+/- (p=0.002, n=3) and Cx32def mice (n=2) compared to untreated mutants (n=3-5). No significant change occurred in wild type and PMP22tg mice n=3. **C)** Regeneration clusters, typical hallmarks of the Cx32def neuropathy became considerably more frequent in CSF-1R inhibitor treated animals (n=2) compared to untreated littermates (n=5).

As a last step in the analysis of axonal properties a limited number of teased fiber preparations available from CSF-1R inhibitor treated wild type and PMP22tg mice allowed us to focus on the nodes of Ranvier. Paranodal compartments appeared normal in both genotypes, as reflected by Caspr1 immunostaining **(Figure 15A and B)**. The juxtaparanodal region has been reported to show abnormalities of voltage-gated K+ channel (Kv1.2) staining (Kohl et al., 2010a). Due to the unavailability of the latter antibody we conducted the analysis applying Caspr2, another marker of the juxtaparanodal region, and classified the findings as symmetric (normal), asymmetric or missing Caspr2 immunoreactivity **(Figure 15B)**. The formation of the abnormal, especially missing Caspr2 domains was only mildly elevated in PMP22tg mice compared to wild type animals. The low sample number (2-3) did not allow a detailed statistical analysis; however, CSF-1R inhibitor treatment did not seem to have a major affect on this aspect of axonal pathology in wild type and PMP22tg mice **(Figure 15C)**.

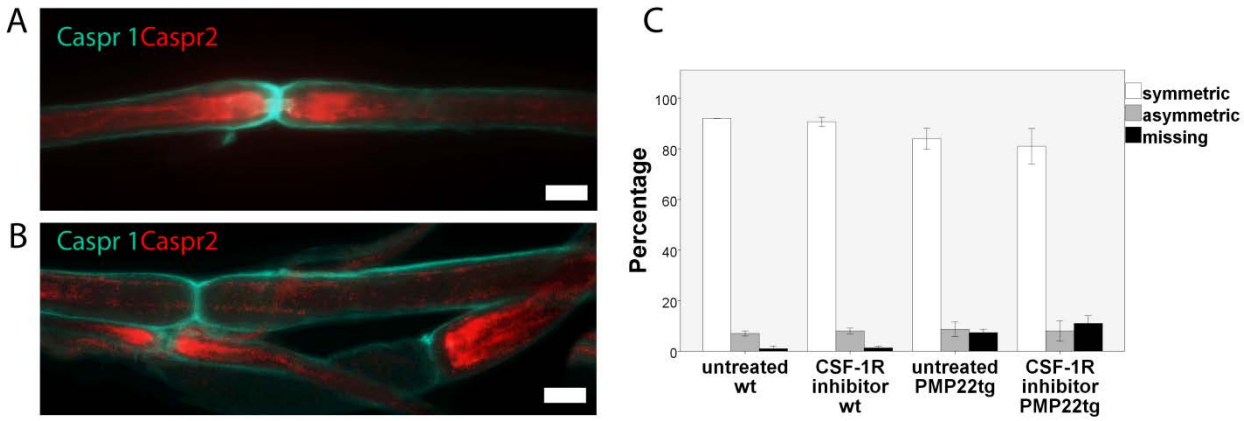

Figure 15. Nodes of Ranvier in CSF-1R inhibitor treated mice.

A) and B) Distribution of Caspr1, a paranodal marker and Caspr2, a juxtaparanodal marker on teased fiber preparations of CSF-1R inhibitor treated (from 3 months up to 6 months of age) wild type and PMP22tg mice. Bar=10 µm **A)** Double immunohistochemistry against Caspr1 and Caspr2 revealing an example of normal, symmetric Caspr2 distribution. **B)** A representative image of symmetric, asymmetric and missing Caspr2 staining found in close proximity on fibers of a CSF-1R inhibitor treated wild type mouse. **C)** Quantification of Caspr2 distribution. PMP22tg mice showed only minor changes compared to wild type littermates. CSF-1R inhibition did not alter Caspr2 distribution profoundly. n=2-3.

3.8. Preliminary data from PMP22tg mice treated with CSF-1R inhibitor from 9 months up to 15 months of age

The limited number of PMP22tg mice treated from 9 months up to 15 months of age provided us the first insights into the effects of CSF-1R inhibition on a mouse model of a late, full blown stage of the most common CMT type.

Macrophage numbers were reduced in the quadriceps nerve of CSF-1R inhibitor treated mice **(Figure 16 A)** and ventral roots showed an average macrophage density of 93.77 macrophages/mm^2 that is lower than values of 6 month old untreated animals **(Figure 5)**.

Until now we could not analyze grip test data due to lack of gender matched control.

Neurophysiological results showed an amelioration of the prolonged F wave latency upon CSF-1R inhibition; not only compared to a 15 month old control mouse **(Figure 16C)** but also when put side by side to 6 month old untreated values. Morphometrical evaluation revealed a corresponding improvement in the myelination state of ventral root axons. The percentage of fully myelinated axons increased markedly, less hypermyelinated fibers could be observed and the decrease in the number of demyelinated fibers occurred in parallel with the increase in the number of thinly myelinated fibers; reflecting a shift towards preserved myelin integrity **(Figure 16B)**.

Even though having only a single control mouse available at this age limited our analysis, preliminary data is suggestive of a beneficial effect of CSF-1R inhibitor on the demyelinating phenotype of 15 month old PMP22tg mice.

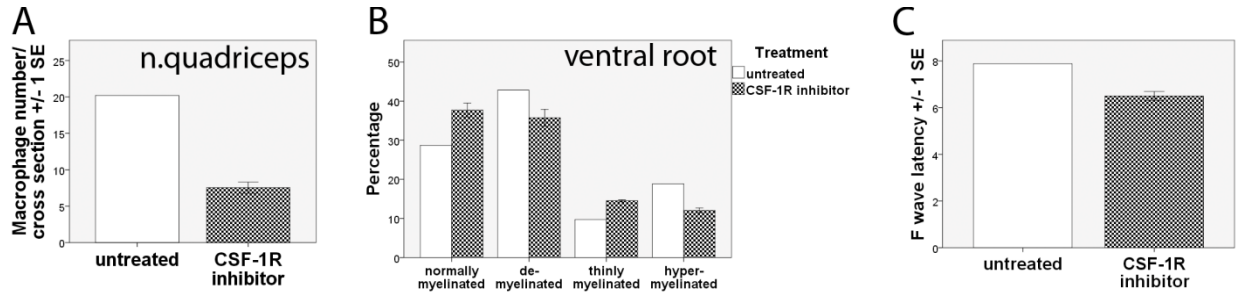

Figure 16.Potential improvement of the demyelinating phenotype in PMP22tg mice treated with CSF-1R inhibitor from 9 months up to 15 months of age.

A) Decreased macrophage numbers in the quadriceps nerve of CSF-1R inhibitor treated PMP22tg mice. n=1-3**B)** Morphometric analysis of the lumbar ventral roots of PMP22tg mice. Note the increased percentage of normally myelinated fibers and the decrease in the number of hypermyelinated axons in CSF-1R inhibitor treated mice. Demyelinated fibers occurred less frequently in treated mice, but the percentage of thinly myelinated fibers increased in the ventral roots. n=1-3. **C)** Reduced F wave latency in treated PMP22tg mice corresponding to the morphological improvement detected in the ventral roots. n=1-3

4. Discussion

4.1. CSF-1 as a potential therapeutic target in CMT

Charcot-Marie-Tooth disease is the most common inherited peripheral neuropathy. Despite the considerable advance in identifying the genetic causes and understanding the pathomechanisms of this disorder during the last decades (Niemann et al., 2006; Reilly and Shy, 2009), therapy is still limited to symptomatic and rehabilitative treatment (Schenone et al., 2011). To date clinical trials failed to prove efficacy of promising candidate drugs, such as vitamin C (Burns et al., 2009b; Micallef et al., 2009; Verhamme et al., 2009; Pareyson et al., 2011), or provided unsatisfactory evidence of improvement in a small number of patients, for example in case of neurotrophins-3 therapy (Pleasure and Chance, 2005). Therefore, identifying further candidate medications is of high importance.

Our group has previously shown the robust beneficial effect of CSF-1 deficiency in mouse models of demyelinating CMT (Carenini et al., 2001; Groh et al., 2012). CSF-1 controls the survival, proliferation, differentiation and function of mononuclear phagocytes. It enhances cytotoxicity, superoxide production, phagocytosis, chemotaxis and cytokine production (Akagawa, 2002). CSF-1 also plays important roles in bone development, fertility, innate immunity, cancer and autoimmune disorders, atherosclerosis and obesity [reviewed in (Chitu and Stanley, 2006)]. Furthermore, secreted and cell-surface isoforms of CSF-1 have distinct effects and are already being studied in the context of CMT in our laboratory.

The effects of CSF-1 are mediated by extracellular binding to the CSF-1R and activation of its intracellular kinase. In our study we applied PLX5622, a low molecular weight inhibitor of the CSF-1R kinase that has already been successfully administered in a phase I clinical trial to rheumatoid arthritis patients. We used pharmacological, high doses of PLX5622 in our study and demonstrate that the blockage of CSF-1 signaling appears to be a promising approach for the treatment of CMT that is however, not devoid of side effects when applied in higher doses.

4.2. CSF-1R inhibitor leads to the reduction of macrophage numbers and improvement of the demyelinating phenotype

The present study confirmed that PLX5622 reached and even exceeded the desired concentration range in PNS tissue and as expected, lead to a prominent decrease in macrophage numbers in the quadriceps nerve of wild type and myelin mutant mice already after 14 days of treatment. Surprisingly, after 3 months of treatment macrophage numbers remained elevated in the quadriceps nerve of Cx32def mice, while a low macrophage number could be observed in the ventral roots of Cx32def mice and in both of the above mentioned PNS tissues of wild type, PMP22tg and P0+/- mice. Cx32 is also absent on the immune cells of Cx32def mutants (Nelles et al., 1996), distinguishing them from the other myelin mutants; however, it is not plausible to assume that resistance to CSF-1R inhibitor is associated with Cx32 deficiency, as macrophage numbers in the ventral roots of Cx32def mice are reduced significantly. We suppose that the distal part of the axon, being far away from the cell body, is highly susceptible to damage in this model of CMT, where untreated animals already show a pronounced axonopathy in addition to the demyelinating phenotype. Moreover, the general absence of Cx32, a gap junction protein, might negatively influence the metabolism of CSF-1R inhibitor contributing to the unfavorable outcome. We hypothesize that treatment initially reduced macrophage numbers and then led to a 'Wallerian degeneration like state' due to its neurotoxic effect, which in turn attracted macrophages to the damaged nerve resulting in high macrophage numbers, similar to those observed in untreated Cx32def mutants. The initial decrease in the macrophage numbers with 14 days of treatment and the increase of quadriceps nerve diameter in treated animals are highly supportive of the above described hypothesis.

Although fibroblast numbers did not change in treated mice; the production of CSF-1, detected by ELISA, showed a several fold increase. In addition, double immunohistochemistry underlined a possible role of fibroblast contact for the survival of macrophages in the presence of CSF-1R inhibitor. A markedly elevated percentage of macrophages were found in close contact with fibroblasts compared to untreated mice. These results further corroborate the findings of the previous study of our group, which showed that the majority of CSF-1 is produced by endoneurial fibroblasts (Groh et al., 2012).

Importantly, along with the decrease in macrophage numbers in the PNS we report a mild, but significant amelioration of the demyelinating phenotype of P0+/- mutants. Moreover, limited evidence suggests similar changes in PMP22tg mice after 6 months of treatment. It is worth noting that elimination of CSF-1 through a genetic approach resulted also in the most pronounced morphologic improvement in the lumbar ventral roots of P0+/- mice (Carenini et al., 2001), corresponding to the data we gained applying a pharmacological inhibitor of CSF-1R. P0+/- mice are relatively mildly affected at 6 months of age and suffer from a progressive neuropathy. Therefore we are encouraged to analyze P0+/- mice that are being treated for a longer period (from 3 months up to 12 months of age) or starting treatment at an older age (treatment from 9 months up to 15 months of age). These experiments will reveal whether the beneficial effects of CSF-1R inhibitor prove persistent and can block or even reverse the progressive segmental demyelination.

Dynamics of the PMP22 neuropathy differ from those of the other two mouse mutants investigated. Myelination occurs almost normally in PMP22tg mice, but they are characterized by increased macrophage numbers and pronounced myelination abnormalities already around 3 to 4 months of age (Kobsar et al., 2005; Barbaria et al., 2009). Their neuropathy remains slowly or nearly non progressive. While PMP22tg mutants treated for 3 months (from 3 months up to 6 months of age) did not show an improvement, mice treated for 6 months (from 9 months up to 15 months of age) revealed a decrease in the percentage of hypermyelinated and demyelinated fibers as well as an increase in the number of thinly myelinated fibers. F waves characterize the properties of proximal segments of the PNS, including the spinal roots. The reduction in prolonged F wave latency reflects the functional significance of the described morphological benefits. These results point out that macrophage numbers need to be constantly reduced for a longer period in order to achieve an improvement or block the progression of demyelination. Based on this preliminary data we are planning to analyze more mice treated for a longer period (either from 3 months up to 12 months or from 9 months up to 15 months of age), especially since these mice are models for the most common form of CMT, and thus represent a principal target group in treatment trials.

Having documented the dramatic and long-lasting improvement in Cx32def osteopetrotic mice (Groh et al., 2012), the lack of improvement in the quadriceps nerve of CSF-1R inhibitor treated Cx32def mice is rather unexpected. Conceivably it can be attributed to the lack of decrease in the macrophage numbers in the quadriceps nerve, or possibly to the enhanced axonopathic changes discussed below. Having ventral root samples from only 2 treated animals available did not allow statistical analysis. Nevertheless, the data is highly similar to the results seen in P0+/- mice. Namely, at 6 months of age the majority of fibers were fully myelinated in the lumbar ventral roots and treatment mildly reduced the proportion of hypo- or demyelinated fibers, suggesting a potential improvement.

4.3. Potential neurotoxic effect of CSF-1R inhibitor treatment

The reduction of CMAP amplitudes called our attention to the effects of CSF-1R inhibitor on axonal characteristics. The deterioration proved to be unambiguous, but affected the distinct mutants to a different degree. In addition, we described morphological correlates of the neurophysiological findings, the decrease in axon numbers of the femoral quadriceps nerve and the shift towards small caliber axons in P0+/- and Cx32def mice, but not in PMP22tg and wt animals.

Wild type animals presented with an approximately 30% reduction of both distal and proximal CMAP amplitudes, which pointed out that the neurotoxic effect of PLX5622 can not only be detected when a myelin mutation renders the peripheral nerves more sensitive to noxious signals. Nevertheless, we could not identify morphological defects in wild type animals. Macrophages are almost completely absent (0-2/cross section) in CSF-1R inhibitor treated wild type animals which might limit fulfilling their physiological role. How this phenomenon affects peripheral nerve integrity is unknown. The number of resident macrophages in the PNS of osteopetrotic mice is normal (Carenini et al., 2001), therefore our previous studies with Cx32def op mutants did not provide insights into possible peripheral nerve alterations that might occur in the absence of macrophages.

Secondary axonopathic changes are well known complications in demyelinating forms of CMT and can be functionally assessed by the reduction in CMAP amplitudes. Most importantly, in CMT1A patients CMAP amplitudes and not NCVs correlate with clinical disability (Krajewski et al., 2000). Therefore, preserving axon integrity is essential in order to achieve a favorable outcome in new treatment approaches.

Cx32def mice provide an ideal model for secondary axonal damage. Already at 6 months of age, the presence of numerous periaxonal vacuoles, regeneration clusters and enlarged periaxonal collars signal ongoing axonal pathology. All pathological alterations except for periaxonal collars are reduced in number in Cx32def op mice as well as denervation of NMJ is substantially attenuated (Groh et al., 2012). These data indicate that the lack of CSF-1 is not only beneficial for diminishing myelination deficits, but influences indirectly axon integrity in a positive way.

The complexity of the axonopathic phenotype must also be kept in mind when analyzing the myelin mutants. CSF-1R inhibitor treated PMP22tg mice presented with a minimal deterioration of CMAP amplitudes compared to untreated littermates and no morphological alteration referring to increased axonal damage. In contrast, treated P0+/- and Cx32def mice showed evidence of axonopathy by both neurophysiologic and morphologic criteria. The combination of reduction in axon number and the absence of large caliber axons might at least partially explain the reduction of CMAP amplitudes in P0+/- and Cx32def mice, but plausible reasons for the electrophysiological changes seen in wild type animals have not been elucidated so far. Differences in the individual mutant strains may be due to a balance shifted towards either a neuroprotective effect coupled with the inhibition of CSF-1 pathway or an equilibrium tilted towards a neurotoxic effect of CSF-1R inhibitor.

Regeneration clusters in Cx32def mice became numerous with CSF-1R inhibitor treatment. We cannot exclude the effect of mixed background on this phenomenon; however, we did not find significant differences in neurophysiological parameters of Cx32def mice having a C57/BL6 or a mixed background, which supports comparable axonal characteristics. Therefore we speculate that the prominent increase in the proportion of regeneration clusters reflects an amplified regeneration effect, trying to maintain proper function and compensate for the loss of fibres in

the quadriceps nerve due in part to CSF-1R inhibitor treatment. Occasional cluster formation was also observed in treated 15 month old PMP22tg mice; nevertheless more animals are needed to properly quantify their presence in CSF-1R inhibitor treated versus untreated mice.

A fascinating compartment for the evaluation of the dual effect of PLX5622 would be the neuromuscular junction. First of all, it should be investigated whether macrophage numbers are reduced in this compartment, especially in Cx32def animals. Lack of CSF-1 leads to improved innervation of the end plates in Cx32def osteopetrotic mice (see above) (Groh et al., 2012). In contrast the reduction in CMAP amplitudes and axon numbers in CSF-1R inhibitor treated mice would suggest a deterioration of the dying back neuropathy in P0+/- and Cx32def animals.

What is the mechanism of neurotoxicity associated with PLX5622 treatment? The first question that arises is: on which structures of the nervous system is CSF-1R expressed. Immunohistochemical and in situ hybridization studies of Wang and colleagues describe that CSF-1R is not or weakly expressed in only a few neurons in steady state conditions in most areas of the brain, but present constitutively in the cerebellum, brainstem, and spinal cord in a greater numbers of neurons (Wang et al., 1999). Spinal cord expression could be relevant in the context of our study and could be confirmed using mice that express GFP coupled CSF-1R. However, the paper describing MacGreen mice did not mention the presence of CSF-1R in the PNS (Sasmono et al., 2003). Even if this could be confirmed, elucidating the mechanism, how CSF-1R blockage in neurotoxicity results, would require additional investigation. Luo and colleagues offer a conceivable explanation, describing the expression of CSF-1R on injured neurons and a protective effect mediating neuronal survival (Luo et al., 2010). A further possibility is that not the blockage of CSF-1R, but the drug itself is neurotoxic. A recent review provides a thorough summary of a large number of studies dealing with the molecular mechanism and therapeutic applications of CSF-1R inhibition (Hume and MacDonald, 2012), without mentioning neurotoxicity. Lastly, mutations in CSF-1R gene have not only been associated with myeloid malignancy (gain of function mechanism) (Ridge et al., 1990), but also with hereditary diffuse leukoencephalopathy (partial loss function mechanism) with spheroids, revealing that defects of macrophage proliferation and differentiation may indirectly lead to a white matter disease (Rademakers et al., 2012).

4.4. Schwann cell – axon interaction, implications in CMT

Schwann cell–axon interactions are indispensable for normal axonal function and as discussed above, are damaged in demyelinating CMT leading to considerable disability in patients (Krajewski et al., 2000). Consequently, analyzing this interaction and developing strategies to preserve it, is essential.

The nodes of Ranvier are specific sites of axon-Schwann cell contact that enable saltatory conduction. Nevertheless, the latter is not the sole advantage of myelination. It also reduces energy consumption considerably by restricting action potentials and ion currents to less than 0,5% of the axon's surface [reviewed in (Nave, 2010a)]. Accordingly, demyelination increases the energy demands. The exposure of voltage gated potassium channels (Kv1.1 and Kv1.2) to the axolemma is a common and early feature of demyelination, causing potassium ions to leak down their concentration gradient, and making it more difficult for depolarisation to occur at the node of Ranvier (Waxman, 2004). However, axonal energy demands are not limited to the nodes of Ranvier, as neuronal ATPases that use most axonal ATP are present along the entire internodal membrane [reviewed in (Nave, 2010b)]. Our group has indeed documented that abnormal ion channel distribution occurs at the nodes of Ranvier in myelin mutants (Ulzheimer et al., 2004; Kohl et al., 2010a; Moldovan et al., 2011; Groh et al., 2012). In the current study we took a closer look at quadriceps nerve teased fiber preparations of CSF-1R inhibitor treated mice. The nodal and paranodal regions, as labeled by the sodium channel Nav1.6 and Caspr1 respectively, appeared normal in 6 month old untreated PMP22tg mice. Conversely, abnormal Kv1.2 potassium channel distribution, including asymmetric and missing immunolabeling could often be found in PMP22tg mutants, while wild type animals showed only occasional maldistribution of Kv1.2 (Kohl et al., 2010a). Unfortunately, the previously used Kv1.2 antibody was no longer available, and therefore we tested another juxtaparanodal marker, Caspr2 (Contactin associated protein 2). This immunostaining also allowed a clear cut categorization of juxtaparanodal regions (symmetric, asymmetric, missing), but showed a much less pronounced difference between wild type and PMP22tg mice and no evidence that CSF-1R inhibitor treatment would aggravate the disorganization of the juxtaparanodal region and contribute to axonal damage this way. The negative finding can be due to the different marker used, Kv1.2 distribution was normal in only

20% of juxtaparanodes of PMP22tg mice, while symmetric Caspr2 staining reached about 80%. Caspr2, an axolemmal cell adhesion molecule might be less prone to damage in the course of demyelination as potassium channels. Interestingly, investigators already considered treating demyelinating neuropathies with potassium channel blockers that would facilitate conduction. Preliminary studies with 3,4 diaminopyridine did not result in significant benefits in CMT patients, most of whom had CMT1 (Russell et al., 1995). However, with more specific potassium channel blockers becoming available, this remains a reasonable approach.

Signaling from axons to Schwann cells could also be manipulated via neuregulin 1 type III (Nrg 1) that determines myelin thickness in the PNS (Michailov et al., 2004). In spite of the attractive theoretical option of increasing myelin thickness in CMT through this pathway, crossbreeding a knock-in mouse model of CMT1B with Nrg1 overexpressing mice did not result in the expected phenotypical improvement (unpublished observations, Patzkó and Shy).

4.5. Prospective therapeutic approaches targeting macrophage mediated detrimental effects in CMT

The current study revealed that the effects of CSF-1R inhibitor treatment are counteracting each other. On one hand along with the decrease of macrophage numbers in the PNS, a promising improvement of the demyelinating phenotype could be detected; on the other hand considerable axonal damage occurred affecting all treated groups. According to mass spectrometry data PLX5622 concentrations exceeded significantly the amount necessary to reduce macrophage numbers. Therefore, the drug concentration should be decreased, which would potentially optimize the effect of the treatment. In our opinion the applied concentration should be high enough to result in a significant reduction of macrophage numbers, but needs to be under the limit that is able to trigger axonopathic changes.

Studying neurodegenerative disorders of the central nervous system might provide insights into potential therapeutic approaches for PNS disorders. To name a few examples, curcumin and fumaric acid has also been applied among others for the treatment of multiple sclerosis (Xie et al., 2011; Gold et al., 2012). Both compounds have a relatively broad spectrum, including

antioxidative and anti-inflammatory properties. They appear to be safe without major side effects and exert their effects at least partially through the inhibition of NF-κB (Sarkar and Li, 2004; Gold et al., 2012).

Curcumin has already been shown to mitigate the phenotype of distinct mouse models of CMT. Khajavi and colleagues provided evidence that curcumin significantly decreased the percentage of apoptotic Schwann cells and increased the number and size of myelinated axons, leading to improved motor performance in TrJ mice (Khajavi et al., 2007). Moreover, oral curcumin treatment not only improved the axonopathic and demyelinating phenotype of the R98C knock-in mouse model of CMT1B, but also promoted Schwann cell myelination, influencing Krox-20, c-Jun and Oct6 expression (Patzkó et al., 2012). In addition, a 12 month dose escalation safety trial has already been conducted in a patient suffering from Dejerine –Sottas syndrome (Burns et al., 2009a). Besides the inhibition of NF-κB, the anti-inflmmatory effect of curcumin is mediated by the suppression of COX-2, IL-1β, IL-6, IL-8 and TNF-α [summarized in (Epstein et al., 2010)]. Taken together these data suggest that the pleiotropic effects of curcumin could also be investigated in the context of the chronic low grade inflammation observed in demyelinating forms of CMT.

Fumaric acid, due to its immunmodulatory potential has recently been used for the treatment of multiple sclerosis and resulted in a reduction of gadolinium enhancing lesions in a phase II clinical trial (Kappos et al., 2008). Fumaric acid was shown to act through the activation of nuclear factor (erythroid-derived 2)-related factor 2 (Nrf2), it enhanced cellular resistance to free radicals by modulating thiols and increasing reduced glutathione levels that lead to the inhibition of nuclear NF-κB translocation (Linker et al., 2011).The combination of neuroprotective and immunmodulatory properties renders fumaric acid to be a potentially attractive candidate for the treatment of CMT.

In conclusion the present study provided evidence that the inhibition of CSF-1R is a suitable and promising approach for the treatment of several forms of demyelinating CMT. However, it also points out an ideal candidate medication should be free of neurotoxic effects. Combination with agents possessing neuroprotective properties could also be considered.

5. Summary

Previous studies by our group revealed that chronic low grade inflammation implicating phagocytosing macrophages is a highly relevant mechanism in the pathogenesis of Charcot-Marie-Tooth disease. The lack of CSF-1, the primary regulator of macrophage function and survival, led to a robust and persistent amelioration of the phenotype in two authentic mouse models of CMT. Moreover, a close contact between CSF-1 producing fibroblasts and endoneurial macrophages carrying CSF-1R has been confirmed in nerve biopsies of CMT patients, further supporting the clinical significance of this pathway.

In the current study we treated 3 distinct mouse models of CMT1: the PMP22tg mice as a model for CMT1A, the P0+/- mice as a model for CMT1B and the Cx32def mice as a model for CMT1X, with a CSF-1R specific kinase (c-FMS) inhibitor (800-1200 mg PLX5622/ kg chow) according to different treatment regimes mimicking an ideal early onset treatment, a late onset treatment and the withdrawal of the drug.

Using the above mentioned doses of PLX5622, we documented a dramatic decrease in macrophage numbers in the PNS of all 3 myelin mutants, except for the quadriceps nerve of Cx32def mice. Fibroblast numbers remained unchanged in treated animals. Surprisingly, in spite of the decrease in the number of detrimental macrophages we could not detect an unequivocal phenotypic improvement. CMAP amplitudes were reduced in both wild type and myelin mutant mice treated with CSF-1R inhibitor in comparison to untreated littermates. Corresponding to the electrophysiological findings, the axon number and the percentage of large diameter axons were reduced in the quadriceps nerve of treated P0+/- and Cx32def mice. By contrast we observed a higher number of fully myelinated axons, in parallel with a decrease in the percentage of demyelinated (and hypermyelinated in PMP22tg mice) fibers in the ventral roots of P0+/- mice treated with CSF-1R inhibitor from 3 months up to 6 months of age and PMP22tg animals treated from 9 months up to 15 months of age.

Our results indicate that CSF-1R inhibitor has the potential to improve the demyelinating phenotype of at least two models of CMT1. Nevertheless, further studies are necessary (for example with lower doses of the inhibitor) to minimize or even eliminate the putative neurotoxic effect we observed with high dose treatment conditions.

6. Zusammenfassung

Vorhergehende Studien unserer Gruppe haben gezeigt, dass eine niedriggradige Entzündung, die von phagozytierenden Makrophagen ausgeht, von ausserordentlicher Bedeutung für die Pathogenese der Charcot-Marie-Tooth Krankheit ist. In Abwesenheit von CSF-1, des primären Regulators für Funktion und Überleben von Makrophagen, trat eine stabile und dauerhafte Verbesserung des Phänotyps in den zwei etablierten CMT Mausmodellen auf. Darüber hinaus konnte ein enger Kontakt zwischen CSF-1-produzierenden Fibroblasten und Makrophagen, die den zugehörigen Rezeptor CSF-1Rexprimieren, in Nervbiopsien von CMT Patienten bestätigt werden, was die klinische Relevanz dieses Mechanismus weiter verdeutlicht.

In der aktuellen Studie wurden drei verschiedene CMT1 Mausmodelle, PMP22tg Mäuse als Modell für CMT1A, P0+/- Mäuse als Modell für CMT1B und Cx32-defiziente Mäuse als Modell für CMT1X, mit einem Inhibitor der CSF-1R spezifischen Kinase (c-FMS) (800-1200 mg PLX5622/kg Futter) behandelt. Der Inhibitor wurde gemäß den verschiedenen Behandlungsmethoden eingesetzt, um den Verlauf einerideal erweise frühzeitigen und einer spät-beginnenden Behandlung und des Entzug des Medikaments zu imitieren.

Nach der Behandlung mit PLX5622 konnten wir im PNS aller drei Myelin-Mutanten, mit Ausnahme des N. quadriceps von Cx32-defizienten Mäusen, einen drastischen Rückgang der Makrophagenanzahl feststellen. Die Anzahl der Fibroblasten blieb in den behandelten Tieren unverändert. Überraschenderweise konnten wir, trotz des Rückgangs der Anzahl an schädlichen Makrophagen, keine einheitliche Verbesserung des Phänotyps dokumentieren. CMAP Amplituden waren nach CSF-1R Inhibitor Behandlung sowohl in Wild-Typ Mäusenals auch in den Myelin-Mutanten geringer als in unbehandelten Kontrolltieren. Passend zu den elektrophysiologischen Ergebnissen war die Anzahl an Axonen und die Prozentzahl an großkalibrigen Axonen im N. quadriceps von behandelten P0+/- und Cx32-defizienten Mäusen reduziert.Im Gegensatz dazu war eine erhöhte Menge an normalmyelinisierten Axonen, mit einer gleichzeitigen Reduktiondemyelinisierter Fasern (und hypermyelinisierten in PMP22tg Mäusen) in den ventralen Spinalwurzeln von P0+/- Mäusen zu beobachten, die mit dem CSF-1R Inhibitor

im Alter von 3 bis 6 Monaten behandelt worden waren sowie bei PMP22tg Mäusen, die im Alter von 9 bis 15 Monaten den Inhibitor erhalten hatten.

Unsere Ergebnisse deuten an, dass der CSF-1R Inhibitor das Potential besitzt, zumindest in zwei Modellen von CMT1 den demyelinisierenden Phänotyp zu verbessern. Dennoch müssen weitere Studien durchgeführt werden (z.B. die Verwendung einer niedrigeren Dosis des Inhibitors), um den möglichen neurotoxischen Effekt, der bei oben genannten Behandlungsbedingungen zu beobachten war, zu minimieren oder ganz zu beheben.

7. Appendix

7.1 Equipment and Materials

7.1.1. Technical equipment

BioPhotometer 6131		Eppendorf (Hamburg, Germany)
Centrifuges:	Biofuge 15R	Heraeus (Hanau, Germany)
	Biofuge pico	Heraeus (Hanau, Germany)
	Centrifuge 5424	Eppendorf (Hamburg, Germany)
Cryostat:	CM 3050S	Leica (Wetzlar, Germany)
Gel chamber (horizontal)		PeqLab (Erlangen, Germany)
Falcon tubes		Greiner (Pleidelsheim, Germany)
Microscopes:	Axiophot 2	Zeiss (Oberkochen, Germany)
	906 E	Zeiss (Oberkochen, Germany)
	TCS SP2 mounted to a DM RE-7 SDK microscope	Leica Microsystems (Wetzlar, Germany)
Object slides superfrost		Langenbrinck (Teningen, Germany)
PapPen		SCI (Munich, Germany)
PCR tubes		Hartenstein (Wuerzburg, Germany)
Pipettes:		Abimed (Berlin, Germany) Eppendorf (Hamburg, Germany) Gilson (Bad Camberg, Germany)
Pipette tips		Sarstedt (Nuembrecht, Germany)
Perfusion pump		“Reglo” Ismatec SA (Glattbrugg-Zuerich)
Power Pac Basic		Biorad (Hercules, CA, USA)
Power Pac 200		Biorad (Hercules, CA, USA)
Program for electrophysiology:		Neruo-MEP (Neurosoft, Ivanovo, Russia)
ProScan Slow Scan CCD camera		Pro Scan (Lagerlechfeld, Germany)
Reactiontubes (0.5ml - 2ml)		Sarstedt (Nuernbrecht, Germany)
Sonoplus HD60		Bandelin Electronic (Berlin, Germany)
Thermocycler: Mastercycler		Eppendorf (Hamburg, Germany)

Primus 96 advanced	PeqLab (Erlangen, Germany)
Thermoshaker TS1	Biometra (Göttingen, Germany)
Ultracut	Leica (Wetzlar, Germany)

7.1.2. Reagents

Acetone	Invitrogen (Karlsruhe, Germany)
Agarose	Sigma (Munich, Germany)
AmpliTaq DNA Polymerase	Applied Biosystems (Darmstadt, Germany)
Aquatex	Merck (Darmstadt, Germany)
Boric acid	Merck (Darmstadt, Germany)
Bovine Serum albumine (BSA)	96 Sigma (Munich, Germany)
Disodium hydrogen phosphate	Merck (Darmstadt, Germany)
Ethanol	J.T. Baker (Deventer, Netherlands)
Ethidiumbromide	Sigma (Munich, Germany)
EDTA	Merck (Darmstadt, Germany)
FCS	Biochrom AG (Berlin, Germany)
Glycine	Sigma (Munich, Germany)
Glycerol	Merck (Darmstadt, Germany)
Heparin	Ratiopharm (Ulm, Germany)
Hepes	Carl Roth (Karlsruhe, Germany)
Ketamin	Medistar(Ascheberg, Germany)
Methanol	J.T.Baker (Deventer, Netherlands)
2-Methylbutane	Carl Roth (Karlsruhe, Germany)
NGS	DAKO (Hamburg, Deutschland)
Nonidet P-40 substitute (NP-40)	Fluka (Buchs, Swiss)
O.C.T. matrix	Hartenstein (Wuerzburg, Germany)
O Range Ruler 600bp DNA ladder	Fermentas (St. Leon-Rot, Germany)
Orange Loading Dye (6x)	Fermentas (St. Leon-Rot, Germany)
Phosphate-buffered saline (PBS)	Biochrom AG (Berlin, Germany)

Primers	Sigma (Munich, Germany)
Potassium di-hydrogen phosphate	Merck (Darmstadt, Germany)
Potassium chloride	Merck (Darmstadt, Germany)
Polyacrylamid	Carl Roth (Karlsruhe, Germany)
Rompun	Bayer HealthCare (Leverkusen, Germany)
Sodium chloride solution	Braun (Melsungen, Germany)
SDS	Carl Roth (Karlsruhe, Germany)
Taq polymerase	Applied Biosystems (Foster City, USA)
TritonX-100	Carl Roth (Karlsruhe, Germany)
Vinyl/ERL4221D	ServaElectrophoresis (Heidelberg, Germany)
Vitro-Clud	Langenbrinck (Teningen, Germany)

7.1.3. Buffers and solutions

Anesthetic:	0.6 ml Ketamin (10%)
	0.2 ml Rompun (2%)
	4.2 ml NaCl (0.9%)
Blocking solution	
for teased fiber preparations:	4% FCS in PBS
	4% NGS in PBS
	0.3 µM Triton
DABCO:	25% 1xPBS
	75% Glycerol
	25mg/ml 1,4-diazabicyclo [2.2.2] octane
	Store at 4°C protected from light.
PBS (1x, pH 7.4):	137mM NaCl
	2.7mM KCl
	1.5mM KH2PO4
	8.1mM Na2HPO4

RIPA lysis buffer (without SDS):	25mM Tris pH 8
	10mM Hepes pH 4.4
	150mM NaCl
	5mM MgCl2
	145mM KCl
	0.4% EDTA
	1% Nonidet P40
	10% Glycerol
	Store at 4°C.
Spurr`s medium:	10g ERL 4206 (3,4-Epoxycyclohexylmethyl-3,4 epoxy- cyclohexylcyclocarboxylate)
	6g DER 736
	26g NSA (Nonenylsuccinicanhydride)
	0.4g DMAE (Dimethylaminoethanol)
TBE (pH 8.0):	89mM Tris
	89mM Borate
	2mM EDTA

Unless otherwise mentioned, distilled water was used as solvent and solutions were stored at room temperature.

7.1.4. PCR conditions, fragment sizes

Mutant	**Cx32def**	**P0+/-**	**PMP22tg**
Primers	0.4 µM	0.29 µM	0.5 µM
dNTP	0.2 µM	0.2 µM	0.2 µM
Taq polymerase	2 U	0.5 U	1 U
$MgCl_2$	0.62 mM		

The PCR was performed in a volume of 50µl with an annealing temperature of 55°C and an elongation temperature of 72°C.

Fragment size	**Cx32:**wt: 550 bp; tg: 414 bp
	P0:wt: 500 bp; tg: 334 bp
	PMP22: wt:450 bp; tg:155 bp

7.1.5. Primer sequences

Mouse mutant	**Primer**	**Sequence**
Cx32def	CxS	5´-CCA TAA GTC AGG TGT AAA GGA GC -3´
	CxAS (wt allel)	5´-AGA TAA GCT GCA GGG ACC ATA GG -3´
	CxNEO(ko allel)	5´-ATC ATG CGA AAC GAT CCT CAT CC -3´
P0 +/-	S 1295	5´-TCA GTT CCT TGT CCC CCG CTC TC-3´
	AS 1772 (wt allel)	5´-ACT TGT CTC TTC TGG GTA ATC AA-3´
	AS 1606 (ko allel)	5´-GGC TGC AGG GTC GCT CGG TGT TC-3´
PMP22tg	MBA1 (wt allel)	5'-AACCGTGAAAAGATGACCC-3'
	MBA2 (wt allel)	5'-TCG TTG CCA ATA GTG ATG ACC-3'
	2F (tg allel)	5'-TCA GGA TAT CTA TCT GAT TCTC-3'
	2R (tg allel)	5'-AAG CTCA TGG AGC ACA AAA CC-3'

7.1.6. Antibodies

Antibodies used for immunohistochemistry				
Primary antibody	**Company**	**Clone**	**Dilution**	**Postfixation**
Mouse anti-rat Caspr1	NIH NeuroMab	75-001	1:300	10 min. aceton
Rabbit anti-mouse CSF1R	Santa Cruz	Sc692	1:100	-
Rabbit anti-rat Caspr2	Millipore	AB5886-500L	1:500	10 min. aceton
Rat-anti-mouse CD34	eBioscience	14-0341-85	1:1000	10 min. aceton
Rat anti-mouse F4/80	Serotec	MCA497	1:300	-
Rat anti-mouse F4/80 Biotin	Serotec	MCA497B	1:300	10 min. aceton

Secondary antibody	Company	Clone	Dilution
Goat anti-mouse Cy2	Dianova	115-225-146	1:300
Goat-anti-rabbit Cy3	Dianova	111-165-144	1:300
Goat anti-rat Alexa Fluor 488	Invitrogen	A11006	1:300
Goat anti-rat Cy3	Dianova	112-165-102	1:300
Streptavidin Cy3	Biozol	CLCSA1010	1:100

7.2 Abbreviations

AARS	alanyl-tRNA synthetase
AD	autosomal dominant
ampl	CMAP amplitude
AR	autosomal recessive
Bp	basis pair
BSA	bovine serum albumin
CMAP	compound muscle action potential
CMT	Charcot-Marie-Tooth disease
Caspr1	Contactin-associated protein 1
Caspr2	Contactin-associated protein 2
CSF-1	Colony stimulating factor 1
CSF-1R	Colony stimulating factor 1 receptor
CTDP1	carboxy-terminal domain, RNA polymerase II, polypeptide A phosphatase, subunit 1
Cx32	Connexin 32
d	distance
def	deficient
dist	distal
dur	duration
DNM2	dynamin 2
EGR2	early growth response2
F	F wave
FCS	fetal calf serum
FGD4	actin-filament binding protein frabin
FIG4	phosphatidylinositol 3,5-bisphosphate 5-phosphatase
GARS	glycyl-tRNA synthetase
GDAP1	ganglioside-induced differentiation-associated protein 1
GJB1	gap junction protein beta 1
H	H reflex

HSP22	22 kDa small heat-shock proteinB8
HSP27	27 kDa small heat-shock proteinB1
Iba1	Ionized calcium binding adaptor molecule 1
lat	latency
LITAF	lipopolysaccharide-induced TNF factor
LMNA	lamin A/C
Mb	mega base (pairs)
MCP-1	monocyte chemotactic protein-1
MFN2	mitofusin-2
MIA	multiple image alignment
min	minute
mm	millimeter
MPZ	myelin protein zero
ms	millisecond
MTMR2	myotubularin related protein 2
MTMR13	myotubularin related protein 13
mV	millivolt
M-CSF	macrophage colony stimulating factor
NCV	nerve conduction velocity
NDRG1	N-myc downstream regulated 1
NEFL	neurofilament light chain
NGS	normal goat serum
Nrf2	nuclear factor (erythroid-derived 2)-related factor
op	osteopetrotic
pers	persistence
PNS	peripheral nervous system
P0	protein zero
PBS	phosphate buffered saline
PMP22	peripheral myelin protein 22
prox	proximal
PRX	periaxin

q.n.	quadriceps nerve
RAG-1	recombination activating gene-1
SBF2	set binding factor 2
SE	standard error
SH3TC2	Src homology 3 domain and tetratricopeptide repeats 2
tg	transgenic
TNF	tumor necrosis factor
TRPV4	transient receptor potential cation channel subfamily V member 4
U	unit
v.r.	ventral root
wt	wild type
YARS	tyrosyl-tRNA synthetase

7.3 References

Adlkofer K, Martini R, Aguzzi A, Zielasek J, Toyka KV, Suter U (1995) Hypermyelination and demyelinating peripheral neuropathy in Pmp22-deficient mice. Nature genetics 11:274-280.

Adlkofer K, Frei R, Neuberg DH, Zielasek J, Toyka KV, Suter U (1997) Heterozygous peripheral myelin protein 22-deficient mice are affected by a progressive demyelinating tomaculous neuropathy. The Journal of neuroscience : the official journal of the Society for Neuroscience 17:4662-4671.

Akagawa KS (2002) Functional heterogeneity of colony-stimulating factor-induced human monocyte-derived macrophages. International journal of hematology 76:27-34.

Anzini P, Neuberg DH, Schachner M, Nelles E, Willecke K, Zielasek J, Toyka KV, Suter U, Martini R (1997) Structural abnormalities and deficient maintenance of peripheral nerve myelin in mice lacking the gap junction protein connexin 32. The Journal of neuroscience : the official journal of the Society for Neuroscience 17:4545-4551.

Barbaria EM, Kohl B, Buhren BA, Hasenpusch-Theil K, Kruse F, Kury P, Martini R, Muller HW (2009) The alpha-chemokine CXCL14 is up-regulated in the sciatic nerve of a mouse model of Charcot-Marie-Tooth disease type 1A and alters myelin gene expression in cultured Schwann cells. Neurobiology of disease 33:448-458.

Berger P, Young P, Suter U (2002) Molecular cell biology of Charcot-Marie-Tooth disease. Neurogenetics 4:1-15.

Berger P, Niemann A, Suter U (2006) Schwann cells and the pathogenesis of inherited motor and sensory neuropathies (Charcot-Marie-Tooth disease). Glia 54:243-257.

Bergoffen J, Scherer SS, Wang S, Scott MO, Bone LJ, Paul DL, Chen K, Lensch MW, Chance PF, Fischbeck KH (1993) Connexin mutations in X-linked Charcot-Marie-Tooth disease. Science 262:2039-2042.

Bernard R, De Sandre-Giovannoli A, Delague V, Levy N (2006) Molecular genetics of autosomal-recessive axonal Charcot-Marie-Tooth neuropathies. Neuromolecular medicine 8:87-106.

Bondurand N, Girard M, Pingault V, Lemort N, Dubourg O, Goossens M (2001) Human Connexin 32, a gap junction protein altered in the X-linked form of Charcot-Marie-Tooth

disease, is directly regulated by the transcription factor SOX10. Human molecular genetics 10:2783-2795.

Brancolini C, Edomi P, Marzinotto S, Schneider C (2000) Exposure at the cell surface is required for gas3/PMP22 To regulate both cell death and cell spreading: implication for the Charcot-Marie-Tooth type 1A and Dejerine-Sottas diseases. Molecular biology of the cell 11:2901-2914.

Brancolini C, Marzinotto S, Edomi P, Agostoni E, Fiorentini C, Muller HW, Schneider C (1999) Rho-dependent regulation of cell spreading by the tetraspan membrane protein Gas3/PMP22. Molecular biology of the cell 10:2441-2459.

Burns J, Joseph PD, Rose KJ, Ryan MM, Ouvrier RA (2009a) Effect of oral curcumin on Dejerine-Sottas disease. Pediatric neurology 41:305-308.

Burns J, Ouvrier RA, Yiu EM, Joseph PD, Kornberg AJ, Fahey MC, Ryan MM (2009b) Ascorbic acid for Charcot-Marie-Tooth disease type 1A in children: a randomised, double-blind, placebo-controlled, safety and efficacy trial. Lancet neurology 8:537-544.

Carenini S, Maurer M, Werner A, Blazyca H, Toyka KV, Schmid CD, Raivich G, Martini R (2001) The role of macrophages in demyelinating peripheral nervous system of mice heterozygously deficient in p0. The Journal of cell biology 152:301-308.

Chance PF, Alderson MK, Leppig KA, Lensch MW, Matsunami N, Smith B, Swanson PD, Odelberg SJ, Disteche CM, Bird TD (1993) DNA deletion associated with hereditary neuropathy with liability to pressure palsies. Cell 72:143-151.

Chitu V, Stanley ER (2006) Colony-stimulating factor-1 in immunity and inflammation. Current opinion in immunology 18:39-48.

Chow CY, Zhang Y, Dowling JJ, Jin N, Adamska M, Shiga K, Szigeti K, Shy ME, Li J, Zhang X, Lupski JR, Weisman LS, Meisler MH (2007) Mutation of FIG4 causes neurodegeneration in the pale tremor mouse and patients with CMT4J. Nature 448:68-72.

Colby J, Nicholson R, Dickson KM, Orfali W, Naef R, Suter U, Snipes GJ (2000) PMP22 carrying the trembler or trembler-J mutation is intracellularly retained in myelinating Schwann cells. Neurobiology of disease 7:561-573.

D'Urso D, Ehrhardt P, Muller HW (1999) Peripheral myelin protein 22 and protein zero: a novel association in peripheral nervous system myelin. The Journal of neuroscience : the official journal of the Society for Neuroscience 19:3396-3403.

D'Urso D, Brophy PJ, Staugaitis SM, Gillespie CS, Frey AB, Stempak JG, Colman DR (1990) Protein zero of peripheral nerve myelin: biosynthesis, membrane insertion, and evidence for homotypic interaction. Neuron 4:449-460.

Dubourg O, Azzedine H, Verny C, Durosier G, Birouk N, Gouider R, Salih M, Bouhouche A, Thiam A, Grid D, Mayer M, Ruberg M, Tazir M, Brice A, LeGuern E (2006) Autosomal-recessive forms of demyelinating Charcot-Marie-Tooth disease. Neuromolecular medicine 8:75-86.

Dyck PJ, Lambert EH (1968) Lower motor and primary sensory neuron diseases with peroneal muscular atrophy. I. Neurologic, genetic, and electrophysiologic findings in hereditary polyneuropathies. Archives of neurology 18:603-618.

England JD, Gronseth GS, Franklin G, Carter GT, Kinsella LJ, Cohen JA, Asbury AK, Szigeti K, Lupski JR, Latov N, Lewis RA, Low PA, Fisher MA, Herrmann DN, Howard JF, Jr., Lauria G, Miller RG, Polydefkis M, Sumner AJ (2009a) Practice Parameter: evaluation of distal symmetric polyneuropathy: role of autonomic testing, nerve biopsy, and skin biopsy (an evidence-based review). Report of the American Academy of Neurology, American Association of Neuromuscular and Electrodiagnostic Medicine, and American Academy of Physical Medicine and Rehabilitation. Neurology 72:177-184.

England JD, Gronseth GS, Franklin G, Carter GT, Kinsella LJ, Cohen JA, Asbury AK, Szigeti K, Lupski JR, Latov N, Lewis RA, Low PA, Fisher MA, Herrmann DN, Howard JF, Jr., Lauria G, Miller RG, Polydefkis M, Sumner AJ (2009b) Practice Parameter: evaluation of distal symmetric polyneuropathy: role of laboratory and genetic testing (an evidence-based review). Report of the American Academy of Neurology, American Association of Neuromuscular and Electrodiagnostic Medicine, and American Academy of Physical Medicine and Rehabilitation. Neurology 72:185-192.

Epstein J, Sanderson IR, Macdonald TT (2010) Curcumin as a therapeutic agent: the evidence from in vitro, animal and human studies. The British journal of nutrition 103:1545-1557.

Fabbretti E, Edomi P, Brancolini C, Schneider C (1995) Apoptotic phenotype induced by overexpression of wild-type gas3/PMP22: its relation to the demyelinating peripheral neuropathy CMT1A. Genes & development 9:1846-1856.

Feely SM, Laura M, Siskind CE, Sottile S, Davis M, Gibbons VS, Reilly MM, Shy ME (2011) MFN2 mutations cause severe phenotypes in most patients with CMT2A. Neurology 76:1690-1696.

Filbin MT, Zhang K, Li W, Gao Y (1999) Characterization of the effect on adhesion of different mutations in myelin P0 protein. Annals of the New York Academy of Sciences 883:160-167.

Filbin MT, Walsh FS, Trapp BD, Pizzey JA, Tennekoon GI (1990) Role of myelin P0 protein as a homophilic adhesion molecule. Nature 344:871-872.

Fischer S, Kleinschnitz C, Muller M, Kobsar I, Ip CW, Rollins B, Martini R (2008) Monocyte chemoattractant protein-1 is a pathogenic component in a model for a hereditary peripheral neuropathy. Molecular and cellular neurosciences 37:359-366.

Giambonini-Brugnoli G, Buchstaller J, Sommer L, Suter U, Mantei N (2005) Distinct disease mechanisms in peripheral neuropathies due to altered peripheral myelin protein 22 gene dosage or a Pmp22 point mutation. Neurobiology of disease 18:656-668.

Giese KP, Martini R, Lemke G, Soriano P, Schachner M (1992) Mouse P0 gene disruption leads to hypomyelination, abnormal expression of recognition molecules, and degeneration of myelin and axons. Cell 71:565-576.

Gold R, Linker RA, Stangel M (2012) Fumaric acid and its esters: an emerging treatment for multiple sclerosis with antioxidative mechanism of action. Clin Immunol 142:44-48.

Groh J, Weis J, Zieger H, Stanley ER, Heuer H, Martini R (2012) Colony-stimulating factor-1 mediates macrophage-related neural damage in a model for Charcot-Marie-Tooth disease type 1X. Brain : a journal of neurology 135:88-104.

Groh J, Heinl K, Kohl B, Wessig C, Greeske J, Fischer S, Martini R (2010) Attenuation of MCP-1/CCL2 expression ameliorates neuropathy in a mouse model for Charcot-Marie-Tooth 1X. Human molecular genetics 19:3530-3543.

Harding AE, Thomas PK (1980a) Genetic aspects of hereditary motor and sensory neuropathy (types I and II). Journal of medical genetics 17:329-336.

Harding AE, Thomas PK (1980b) The clinical features of hereditary motor and sensory neuropathy types I and II. Brain : a journal of neurology 103:259-280.

Houlden H, Girard M, Cockerell C, Ingram D, Wood NW, Goossens M, Walker RW, Reilly MM (2004) Connexin 32 promoter P2 mutations: a mechanism of peripheral nerve dysfunction. Annals of neurology 56:730-734.

Hume DA, MacDonald KP (2012) Therapeutic applications of macrophage colony-stimulating factor-1 (CSF-1) and antagonists of CSF-1 receptor (CSF-1R) signaling. Blood 119:1810-1820.

Huxley C, Passage E, Manson A, Putzu G, Figarella-Branger D, Pellissier JF, Fontes M (1996) Construction of a mouse model of Charcot-Marie-Tooth disease type 1A by pronuclear injection of human YAC DNA. Human molecular genetics 5:563-569.

Huxley C, Passage E, Robertson AM, Youl B, Huston S, Manson A, Saberan-Djoniedi D, Figarella-Branger D, Pellissier JF, Thomas PK, Fontes M (1998) Correlation between varying levels of PMP22 expression and the degree of demyelination and reduction in nerve conduction velocity in transgenic mice. Human molecular genetics 7:449-458.

Ip C, Kroner A, Fischer S, Berghoff M, Kobsar I, Maurer M, Martini R (2006) Role of immune cells in animal models for inherited peripheral neuropathies. Neuromolecular medicine 8:175-190.

Kappos L, Gold R, Miller DH, Macmanus DG, Havrdova E, Limmroth V, Polman CH, Schmierer K, Yousry TA, Yang M, Eraksoy M, Meluzinova E, Rektor I, Dawson KT, Sandrock AW, O'Neill GN (2008) Efficacy and safety of oral fumarate in patients with relapsing-remitting multiple sclerosis: a multicentre, randomised, double-blind, placebo-controlled phase IIb study. Lancet 372:1463-1472.

Khajavi M, Shiga K, Wiszniewski W, He F, Shaw CA, Yan J, Wensel TG, Snipes GJ, Lupski JR (2007) Oral curcumin mitigates the clinical and neuropathologic phenotype of the Trembler-J mouse: a potential therapy for inherited neuropathy. American journal of human genetics 81:438-453.

Kleopa KA, Scherer SS (2006) Molecular genetics of X-linked Charcot-Marie-Tooth disease. Neuromolecular medicine 8:107-122.

Kleopa KA, Yum SW, Scherer SS (2002) Cellular mechanisms of connexin32 mutations associated with CNS manifestations. Journal of neuroscience research 68:522-534.

Kobsar I, Maurer M, Ott T, Martini R (2002) Macrophage-related demyelination in peripheral nerves of mice deficient in the gap junction protein connexin 32. Neuroscience letters 320:17-20.

Kobsar I, Hasenpusch-Theil K, Wessig C, Muller HW, Martini R (2005) Evidence for macrophage-mediated myelin disruption in an animal model for Charcot-Marie-Tooth neuropathy type 1A. Journal of neuroscience research 81:857-864.

Kobsar I, Berghoff M, Samsam M, Wessig C, Maurer M, Toyka KV, Martini R (2003) Preserved myelin integrity and reduced axonopathy in connexin32-deficient mice lacking the recombination activating gene-1. Brain : a journal of neurology 126:804-813.

Kohl B, Fischer S, Groh J, Wessig C, Martini R (2010a) MCP-1/CCL2 modifies axon properties in a PMP22-overexpressing mouse model for Charcot-Marie-tooth 1A neuropathy. The American journal of pathology 176:1390-1399.

Kohl B, Groh J, Wessig C, Wiendl H, Kroner A, Martini R (2010b) Lack of evidence for a pathogenic role of T-lymphocytes in an animal model for Charcot-Marie-Tooth disease 1A. Neurobiology of disease 38:78-84.

Krajewski KM, Lewis RA, Fuerst DR, Turansky C, Hinderer SR, Garbern J, Kamholz J, Shy ME (2000) Neurological dysfunction and axonal degeneration in Charcot-Marie-Tooth disease type 1A. Brain : a journal of neurology 123 (Pt 7):1516-1527.

Lewis RA, Shy ME (1999) Electrodiagnostic findings in CMTX: a disorder of the Schwann cell and peripheral nerve myelin. Annals of the New York Academy of Sciences 883:504-507.

Li J, Krajewski K, Shy ME, Lewis RA (2002) Hereditary neuropathy with liability to pressure palsy: the electrophysiology fits the name. Neurology 58:1769-1773.

Lin H, Lee E, Hestir K, Leo C, Huang M, Bosch E, Halenbeck R, Wu G, Zhou A, Behrens D, Hollenbaugh D, Linnemann T, Qin M, Wong J, Chu K, Doberstein SK, Williams LT (2008) Discovery of a cytokine and its receptor by functional screening of the extracellular proteome. Science 320:807-811.

Linker RA, Lee DH, Ryan S, van Dam AM, Conrad R, Bista P, Zeng W, Hronowsky X, Buko A, Chollate S, Ellrichmann G, Bruck W, Dawson K, Goelz S, Wiese S, Scannevin RH, Lukashev M, Gold R (2011) Fumaric acid esters exert neuroprotective effects in

neuroinflammation via activation of the Nrf2 antioxidant pathway. Brain : a journal of neurology 134:678-692.

Luo J, Pickford F, Britschgi M, Narasimhan R, Alabsi H, Villeda S, Ding Z, Zhang H, Wilson M, Wong G, Relton J, Pollard JW, Wyss-Coray T (2010) Macrophage colony-stimulating factor (M-CSF) receptor is expressed in injured neurons and mediates survival and proliferation. 2010 Neuroscience Meeting Planner San Diego, CA: Society for Neuroscience, Online.

Lupski JR, de Oca-Luna RM, Slaugenhaupt S, Pentao L, Guzzetta V, Trask BJ, Saucedo-Cardenas O, Barker DF, Killian JM, Garcia CA, Chakravarti A, Patel PI (1991) DNA duplication associated with Charcot-Marie-Tooth disease type 1A. Cell 66:219-232.

Magyar JP, Martini R, Ruelicke T, Aguzzi A, Adlkofer K, Dembic Z, Zielasek J, Toyka KV, Suter U (1996) Impaired differentiation of Schwann cells in transgenic mice with increased PMP22 gene dosage. The Journal of neuroscience : the official journal of the Society for Neuroscience 16:5351-5360.

Mandich P, Mancardi GL, Varese A, Soriani S, Di Maria E, Bellone E, Bado M, Gross L, Windebank AJ, Ajmar F, Schenone A (1999) Congenital hypomyelination due to myelin protein zero Q215X mutation. Annals of neurology 45:676-678.

Martini R, Fischer S, Lopez-Vales R, David S (2008) Interactions between Schwann cells and macrophages in injury and inherited demyelinating disease. Glia 56:1566-1577.

Martini R, Zielasek J, Toyka KV, Giese KP, Schachner M (1995) Protein zero (P0)-deficient mice show myelin degeneration in peripheral nerves characteristic of inherited human neuropathies. Nature genetics 11:281-286.

Meier C, Dermietzel R, Davidson KG, Yasumura T, Rash JE (2004) Connexin32-containing gap junctions in Schwann cells at the internodal zone of partial myelin compaction and in Schmidt-Lanterman incisures. The Journal of neuroscience : the official journal of the Society for Neuroscience 24:3186-3198.

Menichella DM, Arroyo EJ, Awatramani R, Xu T, Baron P, Vallat JM, Balsamo J, Lilien J, Scarlato G, Kamholz J, Scherer SS, Shy ME (2001) Protein zero is necessary for E-cadherin-mediated adherens junction formation in Schwann cells. Molecular and cellular neurosciences 18:606-618.

Meyer zu Horste G, Prukop T, Liebetanz D, Mobius W, Nave KA, Sereda MW (2007) Antiprogesterone therapy uncouples axonal loss from demyelination in a transgenic rat model of CMT1A neuropathy. Annals of neurology 61:61-72.

Micallef J et al. (2009) Effect of ascorbic acid in patients with Charcot-Marie-Tooth disease type 1A: a multicentre, randomised, double-blind, placebo-controlled trial. Lancet neurology 8:1103-1110.

Michailov GV, Sereda MW, Brinkmann BG, Fischer TM, Haug B, Birchmeier C, Role L, Lai C, Schwab MH, Nave KA (2004) Axonal neuregulin-1 regulates myelin sheath thickness. Science 304:700-703.

Moldovan M, Alvarez S, Pinchenko V, Klein D, Nielsen FC, Wood JN, Martini R, Krarup C (2011) Na(v)1.8 channelopathy in mutant mice deficient for myelin protein zero is detrimental to motor axons. Brain : a journal of neurology 134:585-601.

Nave KA (2010a) Myelination and support of axonal integrity by glia. Nature 468:244-252.

Nave KA (2010b) Myelination and the trophic support of long axons. Nature reviews Neuroscience 11:275-283.

Navon R, Seifried B, Gal-On NS, Sadeh M (1996) A new point mutation affecting the fourth transmembrane domain of PMP22 results in severe de novo Charcot-Marie-Tooth disease. Human genetics 97:685-687.

Nelis E et al. (1996) Estimation of the mutation frequencies in Charcot-Marie-Tooth disease type 1 and hereditary neuropathy with liability to pressure palsies: a European collaborative study. European journal of human genetics : EJHG 4:25-33.

Nelles E, Butzler C, Jung D, Temme A, Gabriel HD, Dahl U, Traub O, Stumpel F, Jungermann K, Zielasek J, Toyka KV, Dermietzel R, Willecke K (1996) Defective propagation of signals generated by sympathetic nerve stimulation in the liver of connexin32-deficient mice. Proceedings of the National Academy of Sciences of the United States of America 93:9565-9570.

Niemann A, Berger P, Suter U (2006) Pathomechanisms of mutant proteins in Charcot-Marie-Tooth disease. Neuromolecular medicine 8:217-242.

Notterpek L, Ryan MC, Tobler AR, Shooter EM (1999) PMP22 accumulation in aggresomes: implications for CMT1A pathology. Neurobiology of disease 6:450-460.

Pareek S, Notterpek L, Snipes GJ, Naef R, Sossin W, Laliberte J, Iacampo S, Suter U, Shooter EM, Murphy RA (1997) Neurons promote the translocation of peripheral myelin protein 22 into myelin. The Journal of neuroscience : the official journal of the Society for Neuroscience 17:7754-7762.

Pareyson D, Scaioli V, Laura M (2006) Clinical and electrophysiological aspects of Charcot-Marie-Tooth disease. Neuromolecular medicine 8:3-22.

Pareyson D, Reilly MM, Schenone A, Fabrizi GM, Cavallaro T, Santoro L, Vita G, Quattrone A, Padua L, Gemignani F, Visioli F, Laura M, Radice D, Calabrese D, Hughes RA, Solari A (2011) Ascorbic acid in Charcot-Marie-Tooth disease type 1A (CMT-TRIAAL and CMT-TRAUK): a double-blind randomised trial. Lancet neurology 10:320-328.

Passage E, Norreel JC, Noack-Fraissignes P, Sanguedolce V, Pizant J, Thirion X, Robaglia-Schlupp A, Pellissier JF, Fontes M (2004) Ascorbic acid treatment corrects the phenotype of a mouse model of Charcot-Marie-Tooth disease. Nature medicine 10:396-401.

Patzkó Á (2012) Hereditary neuropathies. In: Elsevier First Consult.

Patzkó Á, Bai Y, Saporta M, Katona I, Wu X, Vizzuso D, Feltri ML, Wang S, Dillon L, Kamholz J, Kirschner D, Sarkar FH, Wrabetz L, Shy M (2012) Curcumin derivatives promote Schwann cell differentiation and improve the phenotype of the R98C CMT1B mouse. Brain. 2012 Dec; 135(Pt 12): 3551-66

Paulson HL, Garbern JY, Hoban TF, Krajewski KM, Lewis RA, Fischbeck KH, Grossman RI, Lenkinski R, Kamholz JA, Shy ME (2002) Transient central nervous system white matter abnormality in X-linked Charcot-Marie-Tooth disease. Annals of neurology 52:429-434.

Pennuto M, Tinelli E, Malaguti M, Del Carro U, D'Antonio M, Ron D, Quattrini A, Feltri ML, Wrabetz L (2008) Ablation of the UPR-mediator CHOP restores motor function and reduces demyelination in Charcot-Marie-Tooth 1B mice. Neuron 57:393-405.

Pleasure DE, Chance PF (2005) Neurotrophin-3 therapy for Charcot-Marie-Tooth disease type 1A. Neurology 65:662-663.

Previtali SC, Quattrini A, Fasolini M, Panzeri MC, Villa A, Filbin MT, Li W, Chiu SY, Messing A, Wrabetz L, Feltri ML (2000) Epitope-tagged P(0) glycoprotein causes Charcot-Marie-Tooth-like neuropathy in transgenic mice. The Journal of cell biology 151:1035-1046.

Rademakers R et al. (2012) Mutations in the colony stimulating factor 1 receptor (CSF1R) gene cause hereditary diffuse leukoencephalopathy with spheroids. Nature genetics 44:200-205.

Raeymaekers P, Timmerman V, Nelis E, De Jonghe P, Hoogendijk JE, Baas F, Barker DF, Martin JJ, De Visser M, Bolhuis PA, et al. (1991) Duplication in chromosome 17p11.2 in Charcot-Marie-Tooth neuropathy type 1a (CMT 1a). The HMSN Collaborative Research Group. Neuromuscular disorders : NMD 1:93-97.

Reilly MM, Shy ME (2009) Diagnosis and new treatments in genetic neuropathies. Journal of neurology, neurosurgery, and psychiatry 80:1304-1314.

Ridge SA, Worwood M, Oscier D, Jacobs A, Padua RA (1990) FMS mutations in myelodysplastic, leukemic, and normal subjects. Proceedings of the National Academy of Sciences of the United States of America 87:1377-1380.

Roux KJ, Amici SA, Fletcher BS, Notterpek L (2005) Modulation of epithelial morphology, monolayer permeability, and cell migration by growth arrest specific 3/peripheral myelin protein 22. Molecular biology of the cell 16:1142-1151.

Russell JW, Windebank AJ, Harper CM, Jr. (1995) Treatment of stable chronic demyelinating polyneuropathy with 3,4-diaminopyridine. Mayo Clinic proceedings Mayo Clinic 70:532-539.

Sancho S, Young P, Suter U (2001) Regulation of Schwann cell proliferation and apoptosis in PMP22-deficient mice and mouse models of Charcot-Marie-Tooth disease type 1A. Brain : a journal of neurology 124:2177-2187.

Sarkar FH, Li Y (2004) Cell signaling pathways altered by natural chemopreventive agents. Mutation research 555:53-64.

Sasmono RT, Oceandy D, Pollard JW, Tong W, Pavli P, Wainwright BJ, Ostrowski MC, Himes SR, Hume DA (2003) A macrophage colony-stimulating factor receptor-green fluorescent protein transgene is expressed throughout the mononuclear phagocyte system of the mouse. Blood 101:1155-1163.

Schenone A, Nobbio L, Monti Bragadin M, Ursino G, Grandis M (2011) Inherited neuropathies. Current treatment options in neurology 13:160-179.

Scherer SS, Deschenes SM, Xu YT, Grinspan JB, Fischbeck KH, Paul DL (1995) Connexin32 is a myelin-related protein in the PNS and CNS. The Journal of neuroscience : the official journal of the Society for Neuroscience 15:8281-8294.

Schmid CD, Stienekemeier M, Oehen S, Bootz F, Zielasek J, Gold R, Toyka KV, Schachner M, Martini R (2000) Immune deficiency in mouse models for inherited peripheral neuropathies leads to improved myelin maintenance. The Journal of neuroscience : the official journal of the Society for Neuroscience 20:729-735.

Senderek J, Bergmann C, Weber S, Ketelsen UP, Schorle H, Rudnik-Schoneborn S, Buttner R, Buchheim E, Zerres K (2003) Mutation of the SBF2 gene, encoding a novel member of the myotubularin family, in Charcot-Marie-Tooth neuropathy type 4B2/11p15. Human molecular genetics 12:349-356.

Sereda M, Griffiths I, Puhlhofer A, Stewart H, Rossner MJ, Zimmerman F, Magyar JP, Schneider A, Hund E, Meinck HM, Suter U, Nave KA (1996) A transgenic rat model of Charcot-Marie-Tooth disease. Neuron 16:1049-1060.

Shapiro L, Doyle JP, Hensley P, Colman DR, Hendrickson WA (1996) Crystal structure of the extracellular domain from P0, the major structural protein of peripheral nerve myelin. Neuron 17:435-449.

Shy ME, Arroyo E, Sladky J, Menichella D, Jiang H, Xu W, Kamholz J, Scherer SS (1997) Heterozygous P0 knockout mice develop a peripheral neuropathy that resembles chronic inflammatory demyelinating polyneuropathy (CIDP). Journal of neuropathology and experimental neurology 56:811-821.

Shy ME, Jani A, Krajewski K, Grandis M, Lewis RA, Li J, Shy RR, Balsamo J, Lilien J, Garbern JY, Kamholz J (2004) Phenotypic clustering in MPZ mutations. Brain : a journal of neurology 127:371-384.

Siskind CE, Murphy SM, Ovens R, Polke J, Reilly MM, Shy ME (2011) Phenotype expression in women with CMT1X. Journal of the peripheral nervous system : JPNS 16:102-107.

Skre H (1974) Genetic and clinical aspects of Charcot-Marie-Tooth's disease. Clinical genetics 6:98-118.

Snipes GJ, Suter U, Welcher AA, Shooter EM (1992) Characterization of a novel peripheral nervous system myelin protein (PMP-22/SR13). The Journal of cell biology 117:225-238.

Street VA, Bennett CL, Goldy JD, Shirk AJ, Kleopa KA, Tempel BL, Lipe HP, Scherer SS, Bird TD, Chance PF (2003) Mutation of a putative protein degradation gene LITAF/SIMPLE in Charcot-Marie-Tooth disease 1C. Neurology 60:22-26.

Suter U, Snipes GJ (1995) Biology and genetics of hereditary motor and sensory neuropathies. Annual review of neuroscience 18:45-75.

Suter U, Moskow JJ, Welcher AA, Snipes GJ, Kosaras B, Sidman RL, Buchberg AM, Shooter EM (1992a) A leucine-to-proline mutation in the putative first transmembrane domain of the 22-kDa peripheral myelin protein in the trembler-J mouse. Proceedings of the National Academy of Sciences of the United States of America 89:4382-4386.

Suter U, Welcher AA, Ozcelik T, Snipes GJ, Kosaras B, Francke U, Billings-Gagliardi S, Sidman RL, Shooter EM (1992b) Trembler mouse carries a point mutation in a myelin gene. Nature 356:241-244.

Taylor RA, Simon EM, Marks HG, Scherer SS (2003) The CNS phenotype of X-linked Charcot-Marie-Tooth disease: more than a peripheral problem. Neurology 61:1475-1478.

Tobler AR, Liu N, Mueller L, Shooter EM (2002) Differential aggregation of the Trembler and Trembler J mutants of peripheral myelin protein 22. Proceedings of the National Academy of Sciences of the United States of America 99:483-488.

Ulzheimer JC, Peles E, Levinson SR, Martini R (2004) Altered expression of ion channel isoforms at the node of Ranvier in P0-deficient myelin mutants. Molecular and cellular neurosciences 25:83-94.

Valentijn LJ, Baas F, Wolterman RA, Hoogendijk JE, van den Bosch NH, Zorn I, Gabreels-Festen AW, de Visser M, Bolhuis PA (1992) Identical point mutations of PMP-22 in Trembler-J mouse and Charcot-Marie-Tooth disease type 1A. Nature genetics 2:288-291.

Verhamme C, de Haan RJ, Vermeulen M, Baas F, de Visser M, van Schaik IN (2009) Oral high dose ascorbic acid treatment for one year in young CMT1A patients: a randomised, double-blind, placebo-controlled phase II trial. BMC medicine 7:70.

Verhoeven K, De Jonghe P, Coen K, Verpoorten N, Auer-Grumbach M, Kwon JM, FitzPatrick D, Schmedding E, De Vriendt E, Jacobs A, Van Gerwen V, Wagner K, Hartung HP, Timmerman V (2003) Mutations in the small GTP-ase late endosomal protein RAB7 cause Charcot-Marie-Tooth type 2B neuropathy. American journal of human genetics 72:722-727.

Wang Y, Berezovska O, Fedoroff S (1999) Expression of colony stimulating factor-1 receptor (CSF-1R) by CNS neurons in mice. Journal of neuroscience research 57:616-632.

Warner LE, Hilz MJ, Appel SH, Killian JM, Kolodry EH, Karpati G, Carpenter S, Watters GV, Wheeler C, Witt D, Bodell A, Nelis E, Van Broeckhoven C, Lupski JR (1996) Clinical phenotypes of different MPZ (P0) mutations may include Charcot-Marie-Tooth type 1B, Dejerine-Sottas, and congenital hypomyelination. Neuron 17:451-460.

Waxman SG, Bangalore L. (2004) Electrophysiologic consequences of myelination. In: Myelin biology and disorders (R.A. L, ed), pp 117-143. London: Elsevier.

Xie L, Li XK, Takahara S (2011) Curcumin has bright prospects for the treatment of multiple sclerosis. International immunopharmacology 11:323-330.

Xu W, Manichella D, Jiang H, Vallat JM, Lilien J, Baron P, Scarlato G, Kamholz J, Shy ME (2000) Absence of P0 leads to the dysregulation of myelin gene expression and myelin morphogenesis. Journal of neuroscience research 60:714-724.

Yoshida H, Hayashi S, Kunisada T, Ogawa M, Nishikawa S, Okamura H, Sudo T, Shultz LD (1990) The murine mutation osteopetrosis is in the coding region of the macrophage colony stimulating factor gene. Nature 345:442-444.

Zielasek J, Martini R, Toyka KV (1996) Functional abnormalities in P0-deficient mice resemble human hereditary neuropathies linked to P0 gene mutations. Muscle & nerve 19:946-952.

Zuchner S, Vance JM (2006) Molecular genetics of autosomal-dominant axonal Charcot-Marie-Tooth disease. Neuromolecular medicine 8:63-74.

Danksagung

Mein besonderer Dank gilt Prof. Dr. Rudolf Martini für die Möglichkeit an diesem interessanten Thema forschen zu dürfen.Ich bedanke mich für die mir gebotenen Arbeitsmöglichkeiten in Rahmen seiner Arbeitsgruppe und für seine herausragende menschliche und wissenschaftliche Betreuung.

Weiterhin möchte ich mich auch bei der Firma Plexxikon für die Bereitstellung des CSF-1 Rezeptor Inhibitors und die wissenschaftliche sowie finanzielle Unterstützung bedanken.

Herrn Prof. Michael E. Shy und Herrn Prof. John Kamholz möchte ich für ihre Unterstützung und Begeisterungsfähigkeit danken, womit sie zum ersten Mal mein Interesse im Gebiet peripherer Neuropathien geweckt haben.

Bei Herrn Dr. Wessigbedanke ich mich für die persönliche Betreuung und die lebendigen Diskussionen, welche die zielorientierte und erfolgreiche Weiterentwicklung meiner Projekte ermöglicht haben.

Außerdem danke ich meinen Kollegen Dennis Klein, Janos Groh, Marianne Huber, Susanne Kerscher, Jonas Pausch, Irene Spahn, Jennifer Wettmarshausen, Heinrich Blazyca, Silke Loserth und Bettina Meyer herzlich für die Geduld und Hilfe im Alltag, insbesondere für die herrvorragende Atmosphäre und die anregenden Diskussionen.

Besonderer Dank gebührt Frau Helga Brünner, Herrn Karl-Heinz Aulenbach, Frau Jacqueline Schreiber und Frau Anja Weidner für die Organisation und Pflege der Tiere.

Publikationen:

1. Patzkó Á, Bai Y, Saporta MAC, Katona I, Wu X, Wrabetz L, Wang S, Dillon LM, Kamholz J, Kirschner D, Sarkar F, Shy ME. Curcumin derivatives promote Schwann cell differentiation and improve the phenotype of the R98C knock-in mouse model of CMT1B. Brain 2012: 135; 3551-3166.
2. Saporta MAC, Shy BR, Patzkó Á, Y. Y, Pennuto M, Ferri C, Tinelli E, Saveri P, Kirschner D, Crowther M, Southwood C, Gow A, Wu X, Feltri ML, Wrabetz L, Shy ME. MpzR98C arrests Schwann cell development in a mouse model of early-onset Charcot-Marie-Tooth 1B. Brain 2012: 135; 2032–2047.
3. Miller LJ, Patzkó Á, Lewis RA, Shy ME. Phenotypic presentation of the Ser63del MPZ mutation. JPNS 2012 Jun; 17(2): 197-200
4. Patzkó Á, Shy ME. Charcot-Marie-Tooth Disease And Related Genetic Neuropathies. Continuum: Lifelong Learning in Neurology—Peripheral Neuropathy, Volume 18, Issue 1, February 2012
5. Shy ME, Patzkó Á. Axonal Charcot-Marie-Tooth disease. Curr Opin Neurol 2011 Oct; 24(5):45-83.
6. Patzkó Á, Shy ME. Update on Charcot-Marie –Tooth disease. Curr Neurol Neurosci Rep. 2011 Feb; 11(1):78-88.
7. Patzkó Á, Tóth E, Somogyvári K, Gerlinger I. A comperative clinical study of mucotomy and KTP laser treatment of the inferior turbinate in allergic and non-allergic subjects. Health. 2010 Vol.2 No.11, 1287-1293
8. Trauninger A, Leél-Őssy E, Kamson DO, Pótó L, Aradi M, Kövér F, Imre M, Komáromy H, Erdélyi-Botor S, Patzkó Á, Pfund Z. Risk factors of migraine-related brain white matter hyperintensities: an investigation of 186 patients. J Headache Pain. 2011 Feb;12(1):97-103.
9. Gerlinger I, Török L, Nagy Á, Patzkó Á, Losonczy H, Pytel J. Frequency of coagulopathies in cases with post-tonsillectomy bleeding. Hungarian Medical Journal 2008;149 (10): 441-446
10. Gerlinger I, Fittler A, Mayer A, Patzkó Á, Fónay F, Pytel J, Botz L. Postoperative application of amphotericin B nasal spray in chronic rhinosinusitis with nasal polyposis, with a review of

the antifungal therapy. European Archives of Oto-Rhino-Laryngology 266 (6): 847-855, 2009.

Weitere Publikationen:

1. Patzkó Á, Shy ME. Charcot-Marie-Tooth Disease and Related Genetic Neuropathies. Continuum. Peripheral Neuropathy. February 2012 (18-1)
2. Patzkó Á: Hereditary Neuropathies. Elsevier First Consult (online clinical information tool)

Buchkapitel:

Martini R. Patzkó Á. Neuroglia, 3rd Edition. Chapter 7: Schwann Cells andMyelin

Zusätzlich 7 Vorträge und 13 Poster auf 9 Konferenzen in Deutschland, USA, Australien, Kanada und Italien.